2002) and degradation (Hashimoto *et al.* 1993b; Urai *et al.* 2002) of endogenous D-serine in the brain. The putative serine racemase that synthesizes D-serine from the L-enantiomer has been reported in rodent and human tissues (Wolosker *et al.* 1999). Moreover, a sodium-independent neutral amino acid transporter encoded by *asc-1* displays a high affinity for D-serine as well as L-serine (Fukasawa *et al.* 2000), although D-serine is also taken up into brain tissues in a sodium-dependent manner (Yamamoto *et al.* 2001; Javitt *et al.* 2002; Ribeiro *et al.* 2002).

However, little is known about the exact molecules involved in the metabolic or functional processes involving endogenous brain D-serine. One approach to clarifying these molecules is to identify transcripts that respond to D-serine because neuroactive substances commonly influence the expression of the molecules specifically associated with their metabolism and function. To this end, we have successfully applied a differential cloning technique, RNA arbitrarily primed PCR (RAP–PCR) (Welsh *et al.* 1992), and recently cloned a novel D-serine-, but not L-serine-, responsive transcript, *dsr-1*, from rat neocortex (Tsuchida *et al.* 2001). The predicted *dsr-1* products include a proton-ATPase-like amino acid sequence and are suggested to regulate the uptake or release of D-serine (Tsuchida *et al.* 2001). We have therefore extended the exploration strategy to include other possible key genes in the brain D-serine system.

Materials and methods

Animals and reagents

All animal experiments were performed in strict accordance with the guidance of the Tokyo Medical and Dental University Graduate School, and were approved by the Animal Investigation Committee of the Institute. Male Wistar rats (Clea Japan, Inc., Tokyo, Japan) at postnatal day (PD) 8 (13–20 g) and 50 (200–230 g) were used. The animals were housed at 22.0 ± 0.5°C in a humidity-controlled room under a 12-h light–dark cycle and had free access to food and water.

[α-^{32}P]dCTP and [α-^{32}P]UTP were purchased from Amersham Biosciences Corp. (Piscataway, NJ, USA). D- and L-Serine were purchased from Nacalai Tesque, Inc. (Kyoto, Japan) and dissolved in saline for intraperitoneal (i.p.) injection. For these injection experiments, the rats at PD8 were mainly used because the permeability and accumulation of neutral amino acids in the brain after systemic administration was much less efficient in adult rats compared with that in infant rats, as demonstrated previously (Lefauconnier and Trouve 1983; Takahashi *et al.* 1997; Tsuchida *et al.* 2001). The other chemicals were of ultrapure grade and commercially available.

RNA fingerprinting by RAP–PCR

The rats were received i.p. D- or L-serine (9 mmol/kg bodyweight) dissolved in saline, or saline alone (vehicle) in a volume of 80–120 μL [bodyweight (g) × 6 μl] and killed by cervical dislocation 3 or 15 h later. Because our previous study (Takahashi *et al.* 1997) indicated that systemic administration of a single large dose of D-serine (9 mmol/kg) caused a rapid and linear increase in the neocortical D-serine content until 6 h after injection (steep rise phase) and a constant and prolonged increase in D-serine level from 6 to 15 h after injection (plateau phase), we chose these 3- and 15-h time points as being representative of the two different phases of the increase in D-serine. After i.p. injection, the L-serine content in the neocortex rapidly and dramatically increased, peaked at 3 h, and returned to control level at around 15 h after injection (Takahashi *et al.* 1997).

Following removal of the brain, the cerebral neocortex (dorsal part of the cerebral cortex divided along the rhinal fissure) was rapidly dissected out on ice, immediately frozen in liquid nitrogen and stored at −80°C until use. Total RNA was extracted using the acid guanidinium thiocyanate–phenol–chloroform method (Chomczynski and Sacchi 1987) and converted to single-stranded cDNA by reverse transcriptase with random hexamer primers (SuperScript First-Strand Synthesis System for RT–PCR; Invitrogen Corp., Carlsbad, CA, USA). In preparation of the pooled sample for RNA fingerprinting, eight of an equal amount (40 μl; 1 ng/μl) of the resulting cDNA solution obtained from each rat were combined together in each experimental group (animals treated with D-serine, L-serine or saline for 3 or 15 h). The pooled samples were serially diluted in TE buffer containing 10 mM Tris-Hcl (pH 8.0) 1 mM EDTA and used as a template for PCR using a set of rhodamine-labeled 12-mer arbitrary primers (A63: 5′-CAGGTGTGGGTT-3′; for both the 5′- and 3′-primer). Rhodamine reagent (TAMRA-NHS/DMSO; Applied Biosystems, Foster City, CA, USA) was used to label the 5′-amino-modified oligonucleotide. The reaction was terminated by 0.1 M triethylammonium acetate, and the labeled nucleotide was purified by gel filtration.

The PCR protcol comprised 94°C for 2 min, 40°C for 5 min and 72°C for 5 min for the first cycle; 94°C for 30 s, 40°C for 2 min and 72°C for 1 min for 34 cycles; and then 72°C for 5 min for extension. The PCR products were separated in a 5% denaturing polyacrylamide gel including 7 M urea and 1 × TBE (90 mM Tris-borate and 2 mM EDTA). The cDNA bands separated in the gel were visualized and analyzed using a fluorescence image analyzer (FMBIO II Multi-View; Hitachi Software Engineering Co., Ltd, Tokyo, Japan). The cDNA bands that showed a higher intensity in the D-serine-treated group than in any other group were cut out of the gel. The DNA fragments were re-amplified by a second PCR with the same primer set.

The amplified DNA fragments were cloned using a Thymine and Adenine (TA) cloning vector (pGEM-T Easy vector system; Promega, Madison, WI, USA) and sequenced by ABI Prism 3100 (Applied Biosystems). To determine the full-length structure from the isolated DNA fragments, we performed a rapid amplification of cDNA ends (RACE)–PCR with an aliquot of the oligo-dT selected RNA (1 μg) prepared from the neocortex (SMART RACE cDNA amplification kit; Clontech, La Jolla, CA, USA).

Semiquantitative co-amplification RT–PCR

In experiments with the D- or L-serine, or saline injections, the amount of single-stranded cDNA prepared from the neocortical total RNAs of each rat was individually quantified by co-amplification RT–PCR with an endogenous template as internal standard to further control for variations in sampling and processing between samples (Foley et al. 1993; Lombardo and Brown 1996). 28S rRNA was employed as internal control, because neither D- nor L-serine

affects the expression levels of 28S rRNA (Foley et al. 1993; Tsuchida et al. 2001). In brief, RT was performed using 0.2 μg neocortical total RNA from each animal, and the resulting cDNA was suspended in 10 volumes of TE buffer (pH 8.0) for the PCR template. An appropriate portion (71 or 91% for co-amplification with *dsr-2*) of the added primers specific for the 28S rRNA sequence was phosphorylated at their 3′-ends so that the target and the control exponential phases would overlap. The following primers were used: *dsr-2*, 5′-TGAGCCAGGAATTTAGGAAGGTT-3′ (nt 6187-6209) (5′-primer) and 5′-AGCAAATCTGGCCAAGTCTAATG-3′ (nt 6694-6716) (3′-primer), size of PCR product 530 bp (nt 6187-6716); r28S, 5′-CTCGCTGGCCCTTGAAAATCC-3′ [nucleotides (nt) 2570–2590] (5′-primer) and 5′-CCCAGCCCTTAGAGCCAA TCCTTA-3′ (nt 2719–2742) (3′-primer), size of PCR 173 bp (nt 2570–2742: accession V01270). The PCR parameters used were 94°C for 2 min, 61°C for 3 min and 72°C for 5 min for the first cycle; 94°C for 45 s, 61°C for 2 min and 72°C for 3 min for two cycles; 94°C for 30 s, 61°C for 45 s and 72°C for 1 min for 32 cycles; and then 72°C for 5 min for extension. The PCR products were separated by electrophoresis on 3% NuSieve agarose 3 : 1 gel (FMC Bioproducts, Rockland, ME, USA) in 1 × TAE (40 mm Tris-acetate and 1 mm EDTA). The gel was stained with 0.5 μg/mL ethidium bromide for 30 min. The resulting cDNA bands were visualized by UV irradiation and analyzed quantitatively by measuring the optical density with an image analyzer (Lumi-Imager; Roche Diagnostics, Basel, Switzerland). The relative amount of the *dsr-2* transcript was evaluated as the ratio of the optical density of the *dsr-2* band to that of the 28S rRNA band.

Southern and northern blot analyses

For the Southern blot analysis (Toda *et al.* 2000), genomic DNA purified from the rat cerebral neocortex was digested with restriction enzymes *Bam*HI, *Eco*RI and *Hin*dIII. The resulting DNA fragments (5 μg) were separated in a 1% agarose gel with 1 × TAE and blotted on to a nylon membrane (Hybond-XL; Amersham Biosciences Corp.) by capillary transfer and fixed by UV cross-linking (Hashimoto *et al.* 1998; Toda *et al.* 2000). The membrane was prehybridized at 42°C for 1 h, and subsequently hybridized with the ^{32}P-labeled cDNA probe for *dsr-2* (Megaprime DNA labeling system; Amersham Corp.) in hybridization buffer (Ultrahyb; Ambion, Inc., Austin, TX, USA) at 42°C for 12 h. The hybridized filter was washed in 0.1 × SSC (20 × SSC: 3 M NaCl and 0.3 M sodium citrate) and 0.1% sodium dodecyl sulfate at 60°C for 60 min. For northern blot analysis, poly(A)$^+$ and poly(A)$^-$ RNA from rat cerebral neocortex were purified using a FastTrack 2.0 kit (Invitrogen Corp.), and separated by electrophoresis in a 1% agarose gel containing 6.3% formaldehyde, then blotted on to a nylon membrane by capillary transfer and fixed by UV cross-linking. After prehybridization at 68°C for 1 h, the blotted filter was hybridized with ^{32}P-labeled antisense RNA probes (Riboprobe systems; Promega) corresponding to 1667 bases (nt 4999–6165) of rat *dsr-2* cDNA and 815 bases (nt 1818–2632) of rat neurexin-3α (*nrxn3α*) cDNA at 68°C for 12 h. The filters were washed in 0.1 × SSC and 0.1% sodium dodecyl sulfate at 68°C for 60 min. In these blotting analyses, the washed filters were exposed to an imaging plate and the signals were visualized using a BAS-2500 image analyzer (Fuji Photo Film Co., Ltd, Tokyo, Japan). The probes for the northern blotting procedures were prepared from the pGEM-T Easy vector.

Analysis of genomic structure surrounding *dsr-2* gene

The hybridization screening of the rat genomic RPCI-31 P1-derived Artificial Chromosome (PAC) library was performed with the *dsr-2* cDNA probe used for the Southern blotting (Woon *et al.* 1998; Osoegawa *et al.* 2000). The isolated PAC genomic DNA clone was purified using a large-size plasmid purification kit (NucleoBond BAC100 kit; Macherey-Nagel GmbH and Co. KG, Düren, Germany), sheared into small DNA pieces, and subcloned into the pUC118 vector as a shotgun library. The genomic structure of *dsr-2* was finally obtained as the contigs constructed by the assembly of the random shotgun sequences.

Determination of tissue distribution by RT–PCR

To examine the tissue distribution of the *dsr-2* and neurexin-3α transcripts, we used the cDNA template prepared from various rat tissues (Rat MTC panel I; Clontech Laboratories, Inc., Palo Alto, CA, USA) for RT–PCR (Toda *et al.* 2000). To determine the subregional distribution in the brain and ontogenic changes, total RNA was extracted from each brain region, and reverse transcribed with random hexamer primers as described above. For *dsr-2*, primers were the same as those used for co-amplification PCR. Those for *nrxn3α* were 5′-ATTTGGATGATGGTGGTGTCTGTG-3′ (nt 959–982) (5′-primer) and 5′-TCCTCTCGAGCTTTACTTCTACCT-3′ (nt 1518–1541) (3′-primer), size of PCR product 583 bp (nt 959–1541: accession NM_053817); β-actin, 5′-CTGGGACGATATGGAGAA-GATTTG-3′ (nt 315–338) (5′-primer) and 5′-GGCATCG-GAACCGCTCATTGCCGA-3′ (nt 830–853) (3′-primer), size of PCR product 539 bp (nt 315–853: accession NM_031144); GAPDH, 5′-TGGTGAGTATGTCGTGGAGTCT-3′ (nt 343–364) (5′-primer) and 5′-AATGGGAGTTGCTGTTGAAGTC-3′ (nt 923–944) (3′-primer), size of PCR product 602 bp (nt 343–944: accession BC059110); NMDA receptor NR2B subunit, 5′-ATCGGCCTGCC-CTCCTCCAAACATAGC-3′ (nt 3130–3156) (5′-primer) and 5′-GGGCCCACCTCCACTGACCGAATCTC-3′ (nt 3548–3573) (3′-primer), size of PCR product 444 bp (nt 3130–3573: accession M91562); DAO, 5′-GCTGGGGAACTGGAGCGAGCTAAACAG-3′ (822–848) (5′-primer) and 5′-CTGGGGCTGGGGGAGGGAAT-CATCA-3′ (nt 1204–1229) (3′-primer), size of PCR product 408 bp (nt 822–1229: accession AB003400).

The PCR parameters were as follows: *dsr-2* and neurexin-3α: 94°C for 3 min, 55°C for 2 min and 72°C for 3 min for the first cycle; 94°C for 30 s, 55°C for 1 min and 72°C for 2 min for two cycles; 94°C for 30 s, 55°C for 45 s and 72°C for 90 s for 34 (for *dsr-2*) or 29 (for *nrxn3α*) cycles; and 72°C for 5 min for extension. β-Actin: 94°C for 2 min, 55°C for 3 min and 72°C for 5min for the first cycle; 94°C for 45 s, 55°C for 2 min and 72°C for 3 min for two cycles; 94°C for 30 s, 55°C for 45 s and 72°C for 1 min for 21 cycles; and then 72°C for 5 min for extension. GAPDH: 94°C for 3 min, 55°C for 2 min and 72°C for 3 min for the first cycle; 94°C for 30 s, 55°C for 45 s and 72°C for 3 min for 26 cycles; and then 72°C for 5 min for extension. NR2B: 94°C for 3 min, 60°C for 2 min and 72°C for 3 min for the first cycle; 94°C for 30 s, 60°C for 1 min and 72°C for 90 s for two cycles; 94°C for 30 s, 60°C for 45 s and 72°C for 90 s for 30 cycles; and then 72°C for 5 min for extension. DAO: 94°C for 3 min, 55°C for 2 min and 72°C for 3 min for the first cycle; 94°C for 30 s, 55°C for 1 min and 72°C for 90 s for two cycles; 94°C for 30 s, 55°C for 45 s and 72°C for 90 s for 31 cycles; and then 72°C for 5 min for extension.

Statistical analysis

The results were usually expressed as the mean ± SEM of data obtained from eight determinations. Statistical analyses were performed using one-way ANOVA followed by Scheffé's multiple comparison test.

Results

Isolation of the D-serine transcript *dsr-2*

To identify the transcript that exhibits a response to D-serine, we performed RAP–PCR using neocortical samples prepared from 8-day-old rats, 3 and 15 h after i.p. injection of D- and L-serine (9 mmol/kg) and saline. In previous experiments, we confirmed that these amino acids had efficiently accumulated in the cerebral neocortex at these times after systemic administration (Takahashi *et al.* 1997). Under these conditions, we screened the responsive genes using several arbitrary primers. As shown in Fig. 1(a), using a rhodamine-labelled primer (A63), we detected an amplified DNA band that was enhanced by the injection of D-serine, but not L-serine, at 3 h. The DNA was isolated from the gel, and designated as *dsr-2* (D-serine *r*esponsive transcript-2). Using a semiquantitative co-amplification PCR method with 28S rRNA (Tsuchida *et al.* 2001; Kajii *et al.* 2003), we confirmed that levels of *dsr-2* mRNA in the cerebral neocortex had significantly increased by 3 h after administration of D-serine in a stereoselective manner (Fig. 1b).

Structural analysis of *dsr-2* gene

Based on the structural analysis of cDNA by RACE–PCR and genomic walking, we determined the 7199 bases of the nucleotide sequence of the *dsr-2* cDNA, which consisted of a single exon (Fig. 2). The deduced 111 amino acids of the peptide sequence were predicted by a computer-based open reading frame (ORF) search analysis using the GENETYX program (GENETYX version 7.0; Genetyx Corp., Tokyo, Japan). However, the translational initiation sequence did not satisfy the Kozak consensus sequence. Further investigation is required to confirm the N-terminus of the predicted protein. The above obtained nucleotide sequence has been deposited at the DNA Data Bank of Japan (DDBJ) (Accession No. AB200323).

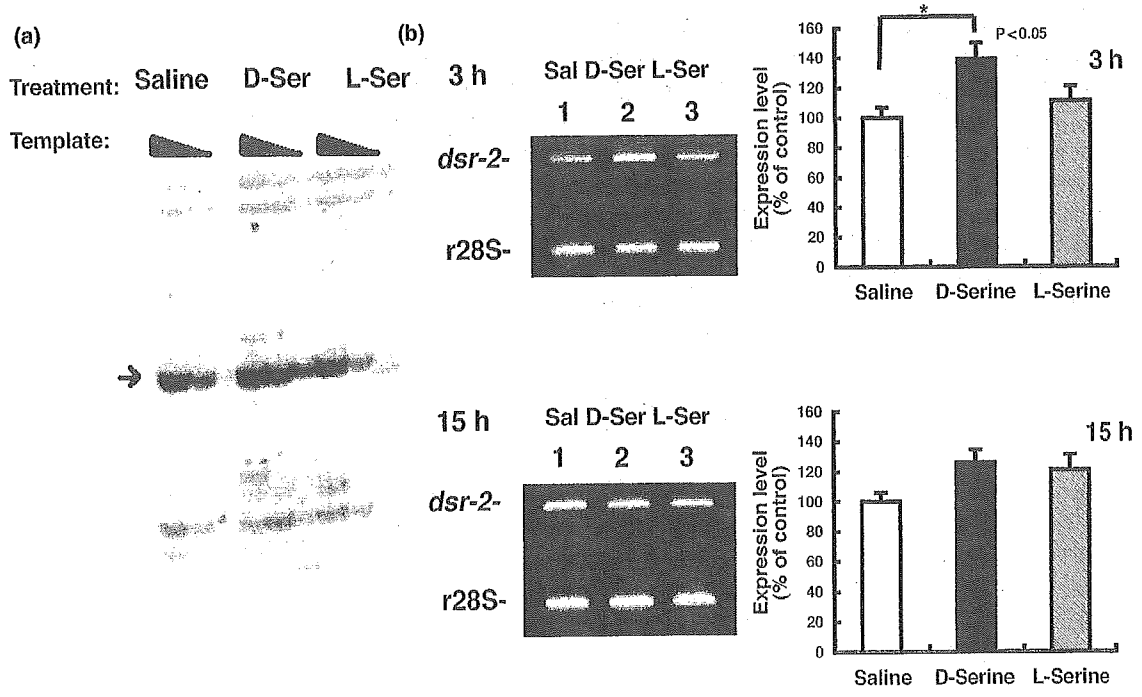

Fig. 1 Isolation of D-serine-regulated transcript *dsr-2* from rat brain. (a) Detection of *dsr-2* in the neocortex of the infant rat 3 h after i.p. injection of D-serine, L-serine or saline by RNA fingerprinting using RAP–PCR. The serially diluted neocortical cDNA templates (concentrations at × 4, × 2 and × 1 from left to right in each group) were amplified with a set of rhodamine-labeled primers of the same sequence (A63: 5′-CAGGTGTGGGTT-3′). The arrow indicates the signal corresponding to the *dsr-2* DNA fragment that was enhanced by D-serine. (b) Effects of systemic administration of D- and L-serine on the expression of *dsr-2* transcript in the neocortex of infant rat. The neocortex was dissected out 3 or 15 h after systemic injection of D- or L-serine, or saline. The level of *dsr-2* was determined quantitatively by the co-amplification RT–PCR method with 28S rRNA as an endogenous control. Representative gel images of the resulting *dsr-2* and r28S bands are shown in the left panel (phosphorylation rate of the r28S primers was 71%). Results are mean ±SEM of eight individual values per experimental group (3-h or 15-h D-serine, L-serine or saline treatment) expressed as a percentage of the respective saline-treated control value [control values: 3 h, 0.87 ± 0.06; 15 h, 1.05 ± 0.06 (phosphorylation rate of the r28S primers was 91%]. *$p < 0.05$ (ANOVA followed by Scheffe's multiple comparison test).

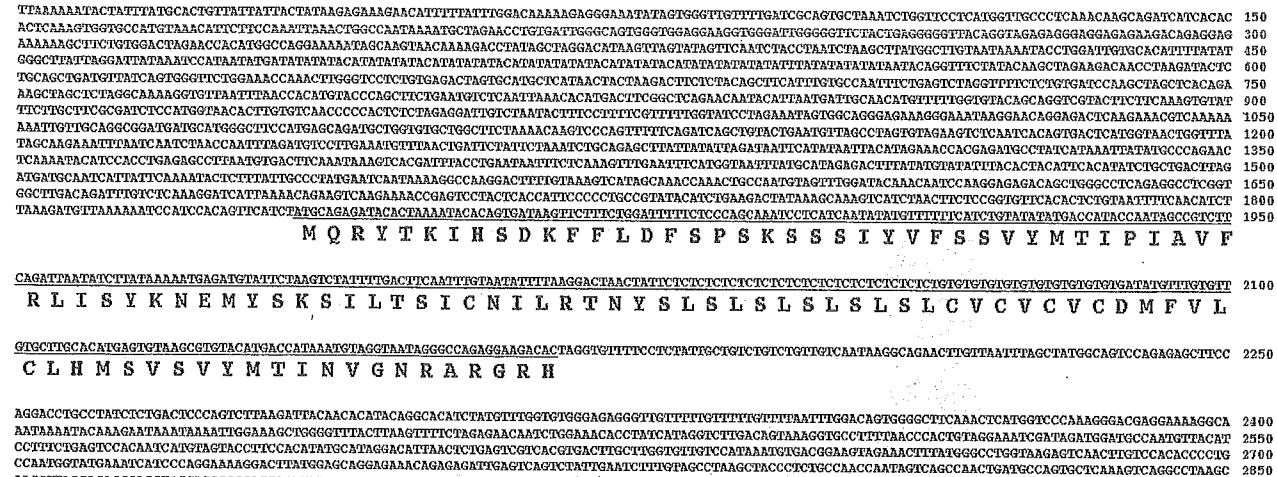

Fig. 2 Nucleotide sequence of *dsr-2* cDNA. The 7199-bp sequence of *dsr-2* cDNA is shown with the deduced amino acid sequence, predicted by the computer-based ORF search analysis using the GENETYX program (GENETYX version 7.0; Genetyx Corp., Tokyo, Japan). The nucleotides contained in the ORF are marked with fine underlines. The nucleotide sequences initially primed by the arbitrary primer A63 are underlined in bold. An atypical poly(A) signal before the poly(A) stretch is indicated as an open box. The nucleotide sequence obtained has been deposited at the DDBJ (Accession no. AB200323).

In Southern blotting using 1667 bases of the cDNA probe for *dsr-2*, we detected a single band at 4.4, 12.7 and 2.3 in the *Bam*HI-, *Eco*RI- and *Hin*dIII-digested genomic DNA of the rat respectively (Fig. 3a). With the same probe, a single band at 9.5 kb was detected in *Eco*RI-digested mouse genomic DNA (data not shown). These results indicate that the *dsr-2* gene exists as a single copy in both the rat and mouse genomes. Using the same cDNA probe, we screened a rat genomic library to clarify the genomic structure surrounding the *dsr-2* gene locus. We isolated a positive clone with an insert size of 176 kb from the rat PAC genomic library (Woon *et al.* 1998) and determined the entire primary structure by shotgun sequencing. These analyses, together with the Basic Local Alignment Search Tool (BLAST) database search of rat genomic DNA, revealed that the *dsr-2* gene maps to the opposite strand of the large intron (354 kb) between exon 5 and exon 6 of the *nrxn3α* gene in rat chromosome 6. The rat *nrxn3α* gene consists of 7009 nucleotides of mRNA, extends to the large range of chromosome 6q24-31 (1.63 Mbp) and has multiple alternative splicing sites. The BLAST search further revealed that the mouse or human homologous nucleotide sequence of the rat *dsr-2* gene also mapped to the opposite strand of the similar large intron of the mouse *nrxn3* gene (NM_172544) on chromosome 12 (NT_039552) or that of the human *nrxn3* gene (NM_004796) on chromosome 14 (NT_086807).

Detection of *dsr-2* mRNA in the CNS

Because the polyadenylation signal of the *dsr-2* transcript was found to be atypical, we examined the mRNA signals by the northern blot analysis, not only in the poly(A)$^+$ RNA fraction but also in the poly(A)$^-$ RNA fraction prepared from the neocortex. With a specific antisense RNA probe for the *dsr-2* transcript constructed from the genomic *dsr-2* sequence, we detected a single band at

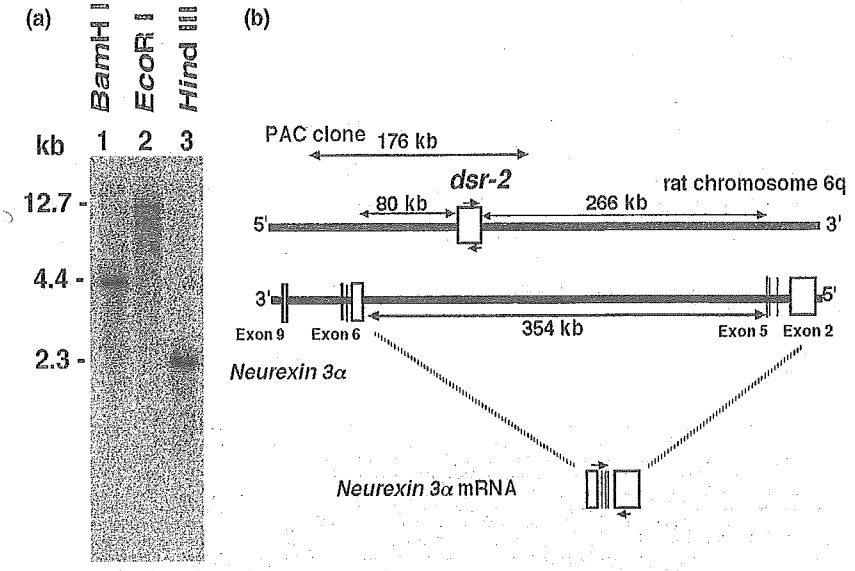

Fig. 3 Genomic organization of *dsr-2*. (a) Southern blot analysis of *dsr-2*. Rat genomic DNA was isolated from adult rat neocortex and digested by one of three restriction enzymes. A single band at 4.4 kb, 12.7 kb and 2.3 kb was detected with the DNA digested by *Bam*HI, *Eco*RI and *Hin*dIII respectively. (b) Genomic structure of *dsr-2* in the rat. The genomic organization of *dsr-2* and *nrxn3α* is illustrated based on the data obtained by DNA sequencing of the corresponding PAC genomic clone and BLAST database analyses. The *dsr-2* gene is located on the reverse strand within a large intron of the *nrxn3α* gene mapped to rat chromosome 6q24-31. The short arrows indicate the positions of primers used for RT–PCR.

7.1 kb in the northern blot analysis of the poly(A)$^+$, but not of the poly(A)$^-$, RNA fraction (Fig. 4a). The size of *dsr-2* transcripts coincided with that of the obtained *dsr-2* cDNA, confirming that the cloned cDNA is full-length. The corresponding sense probe for the *dsr-2* transcript failed to produce any hybridization signals. With the antisense probe for the *nrxn3α* transcript, which is constructed from the opposite strand of the genomic *dsr-2* sequence, a doublet of bands around 9.5 kb was observed (Fig. 4a) as reported previously (Ushkaryov and Südhof 1993). The *nrxn-3* sense probe did not detect any messages from the *dsr-2* strand (Fig. 4a).

Distribution of *dsr-2* transcript in forebrain areas of adult rat

The tissue distribution of *dsr-2* and *nrxn3α* mRNAs was examined in the adult rat (PD50) by RT–PCR (Fig. 4b). Basal expression of the *dsr-2* transcript was exclusively detected in the brain. Basal levels of the *nrxn3α* transcript were detected in the brain and testis. The reliability of the present RT–PCR method was confirmed by the ubiquitous distribution of high levels of β-actin mRNA.

The regional distribution of *dsr-2* mRNA in the brain was examined by RT–PCR assay in the adult rat (Fig. 5a). Expression of the *dsr-2* transcript was predominant in the forebrain (cortex, limbic forebrain, striatum and hippocampus), less in the midbrain (thalamus, hypothalamus and midbrain), and even lower in the hindbrain (pons–medulla and cerebellum). This characteristic distribution closely resembled that of free D-serine in the rat brain as determined

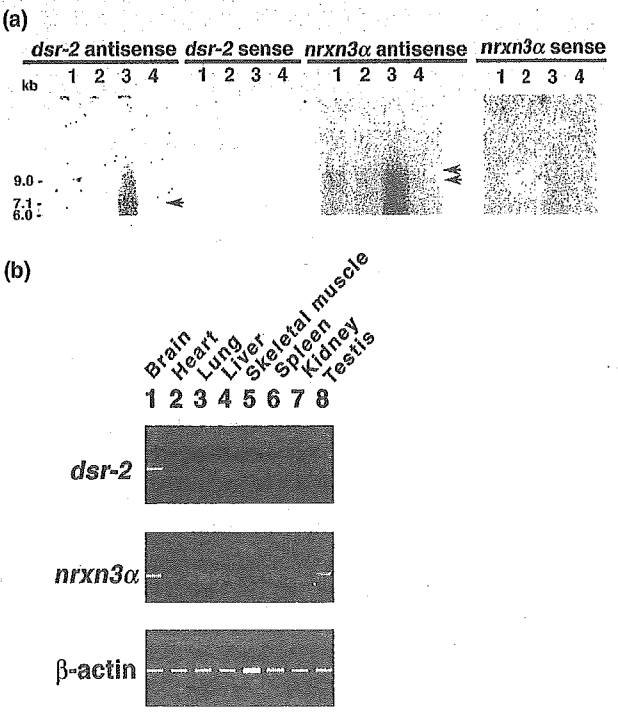

Fig. 4 Expression of *dsr-2* mRNA in brain. (a) Northern blot analysis of *dsr-2* and *nrxn3α*. The mRNA was extracted from adult rat cerebral neocortex and hybridized with *dsr-2* (antisense and sense) and *nrxn3α* (antisense and sense) riboprobes. Lane 1, 10 μg total RNA; lane 2, 2 μg poly(A)$^+$ RNA; lane 3, 20 μg poly(A)$^+$ RNA; lane 4, 10 μg poly(A)$^-$ RNA. The arrows indicate the specific bands detected in the poly(A)$^+$ fraction. (b) Tissue distribution of *dsr-2* and *nrxn3α* transcripts. The basal expression of *dsr-2*, *nrxn3α* and β-actin mRNAs in brain and peripheral tissues was determined by RT–PCR.

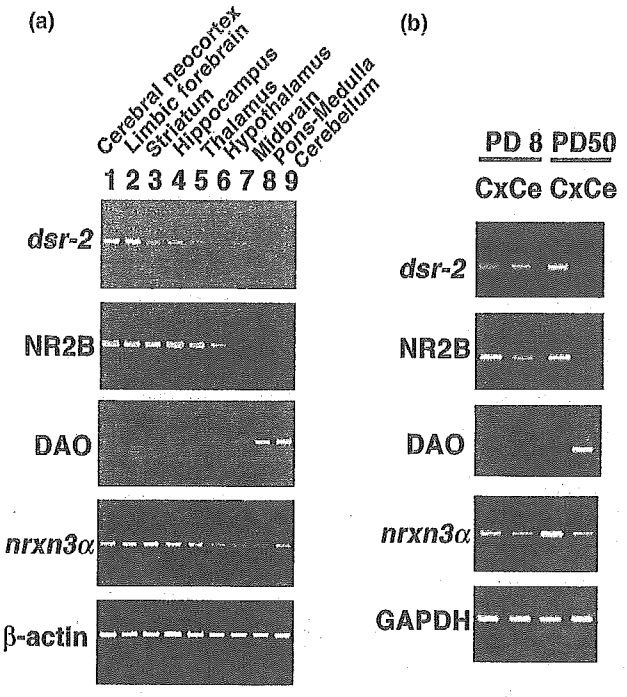

Fig. 5 Ontogenic change in distribution of *dsr-2* transcript in the rat CNS. (a) Subregional distribution of *dsr-2* mRNA in the adult rat brain. The basal expression of *dsr-2*, NR2B, DAO and *nrxn3α* mRNAs was determined semiquantitatively by RT–PCR. (b) Ontogenic changes in the distribution pattern of *dsr-2* mRNA. The basal expression of *dsr-2*, NR2B, DAO and *nrxn3α* mRNAs was determined semiquantitatively by RT–PCR in the infant (PD8) and adult (PD50) rat cerebral neocortex (Cx) and cerebellum (Ce).

by HPLC (Hashimoto *et al.* 1993c) and by immunohistochemistry (Schell *et al.* 1995). Based on previous studies that involved *in situ* hybridization and immunohistochemical analyses (Monyer *et al.* 1992; Nakanishi 1992; Horiike *et al.* 1994), it was speculated that D-serine and the NR2B subunit would display a similar distribution pattern and that DAO would be distributed in a complementary manner to the two molecules. Results of analysis of the distribution of the NR2B and DAO transcripts in various brain areas using RT–PCR supported this presumption (Fig. 5a), suggesting that the *dsr-2* gene product may be involved in synaptic functions regulated by the D-serine/NMDA receptor NR2B-mediated signaling. The basal expression level of the *nrxn3α* transcript was also predominant in the forebrain. However, we detected a relatively large amount of *nrxn3α* mRNA in rat cerebellum. The reliability of the RT–PCR method was verified by the ubiquitous distribution of β-actin mRNA.

Ontogenetic changes in the distribution pattern of *dsr-2* transcript in the rat brain

During development of the rat, endogenous D-serine and the NR2B subunit were both detected transiently (from first to third week after birth) at high levels in the cerebellum (Watanabe *et al.* 1992; Hashimoto *et al.* 1995b; Schell *et al.* 1997). In this study, therefore, the expression of *dsr-2* mRNA was examined in the cerebral neocortex and cerebellum of both infant (PD8) and adult (PD50) rats by RT–PCR. In the infant rat, the cerebellum showed much higher expression of *dsr-2* mRNA than the cerebral neocortex, whereas the adult neocortex and cerebellum showed intense and no detectable expression of the transcript respectively (Fig. 5b). This ontogenic change in the distribution pattern was again similar to that of NR2B mRNA and complementary to that of DAO mRNA. In contrast, there was no change in the distribution pattern of *nrxn3α* mRNA during postnatal development. The fact that no regional and developmental differences were seen in GAPDH mRNA expression attested to the reliability of the RT–PCR method.

Discussion

Using an RNA fingerprinting technique, we isolated a novel and D-serine up-regulated transcript designated as *dsr-2* from the rat neocortex. Systemic administration of D-serine, but not L-serine, enhances the neocortical expression of *dsr-2* mRNA. The *dsr-2* gene is located on the reverse strand within an intron of the *nrxn3α* gene mapped to rat chromosome 6q24-31 and is exclusively transcribed in the brain. The regional distribution of the basal expression of *dsr-2* and its ontogenic changes are closely correlated with those of the free D-serine content and of the NMDA receptor R2B subunit.

Detection of a single band of 7.1 kb by northern blot hybridization with a specific riboprobe for *dsr-2* (Fig. 3a), the RT–PCR results and database search (data not shown) support the view that there are no apparent splicing variants of the *dsr-2* transcript. Sequence analysis of the cloned *dsr-2* cDNA indicates that *dsr-2* mRNA has an ORF that is predicted to encode 111 amino acids. Because the deduced amino acid sequence contains no consensus motifs, the exact physiological significance of the predicted protein remains unclear.

Modification of *dsr-2* expression is likely to be related to NMDA receptor-mediated glutamate transmission because glycine site-mediated facilitation of the NMDA receptor is caused by D-serine. The possible functional link of *dsr-2* with D-serine and NMDA receptors is further supported by the brain-selective and D-serine- and NR2B subunit-like distribution of the basal expression of *dsr-2* in infant and adult rat brains. The pharmacological, neuroanatomical and developmental correlates also indicate that *dsr-2* and its protein product may play a physiological role in control of the metabolism and function of D-serine and NMDA receptors.

Genomic walking, genome library screening and a database search revealed that the entire length of the *dsr-2* gene lies within the opposite DNA strand of the 354-kb intron of the *nrxn3α* gene that encodes highly polymorphic neuron-specific cell-surface proteins involved in the regulation of synaptic neurotransmission (Missler *et al.* 2003). This unique structural

relationship between the two genes, which is conserved in the mouse and human, could reflect their functional association.

The *dsr-2* transcript might act as a natural antisense regulator of *nrxn3α* expression. It has recently been appreciated that changes in mRNA half-life and translation can be mediated not only by RNA-binding proteins but also by sense–antisense RNA interactions (Lehner *et al.* 2002; Carmichael 2003). For instance, translation of the neural nitric oxide synthase protein from its mRNA has been shown to be inhibited by the corresponding antisense region of the pseudogene (Korneev *et al.* 1999; Korneev and O'Shera 2002). The resulting RNA duplex would prevent the sense RNA from interacting with diverse cellular components required for a normal sense expression. Alternatively, the duplex may represent substrates for double-stranded RNA-specific enzymes (Vanhée-Brossollet and Vaquero 1998). Because the DNA sequence of the *dsr-2* gene is complementary to that of a part of the *nrxn3α* intron between its 5 and 6 exons, the *dsr-2* transcript might influence the editing and maturation of premature *nrxn3α* mRNAs by hybridizing to the complementary sequence. However, it is unlikely that the *dsr-2* transcript would solely be a specific antisense regulator of the *nrxn3α* gene, as expression patterns of *dsr-2* and *nrxn3α* mRNAs are not always parallel in the brain and periphery; in adult rats, substantial expression of *nrxn3α*, but not *dsr-2*, mRNA is detected in the cerebellum and testis, whereas the cerebellum exhibits intense expression of these genes during development.

It is also possible that the *dsr-2* RNA might be required for *trans*-splicing variants of *nrxn3α*. *Trans*-splicing is an intermolecular reaction between a splice donor and a splice acceptor in two separate mRNAs (Pirrotta 2002) and has recently been observed in editing mammalian gene transcripts including rat carnitine octanoyltransferase, rat voltage-gated sodium channel and rat Sp1 mRNAs (Caudevilla *et al.* 1998; Akopian *et al.* 1999; Takahara *et al.* 2002). The above possibility is raised by the hypothesis that, in the particular variation upon splicing, the RNAs on opposite strands are independently transcribed but the transcribed regions overlap, therefore resulting in the presence of complementary sequences in the primary transcripts to be *trans*-spliced. A lack of reports of *nrxn3α* variants containing the nucleotide sequence of *dsr-2* and the differential expression of the two genes in the testis and cerebellum, however, argue against the occurrence of *trans*-splicing.

Because the distribution of the mRNA signals of *dsr-2*, NR2B and *nrxn3α* are roughly similar in the brain areas examined, with the exception of the cerebellum, and because α-neurexin (including neurexin-3α)-deficient mice exhibited a decreased NMDA receptor-dependent postsynaptic current (Kattenstroth *et al.* 2004), the sense–antisense transcription in the *dsr-2–nrxn3α* locus is implicated in the regulation of *dsr-2* expression and NMDA receptor-directed D-serine signaling in the brain. Further investigation is needed to clarify these possibilities as well as the physiological role of *dsr-2*; *dsr-2* gene-targeted mice are currently being prepared.

In conclusion, we have demonstrated that rat brain expresses a novel and apparently coding antisense transcript, *dsr-2*, that is induced by D-serine. The D-serine-responsive nature, and brain-selective, D-serine- and NR2B subunit-related distribution, of *dsr-2* mRNA are consistent with the idea that *dsr-2* may participate in the control of D-serine metabolism and function and of NMDA receptor-mediated signaling in the mammalian brain. Genomic analysis indicates that the *dsr-2* mRNA is derived from the opposite strand of an intron of the *nrxn3α* gene, suggesting a regulatory role of sense–antisense transcription in the interactions between *dsr-2*, *nrxn3α*, D-serine and the NMDA receptor.

Acknowledgements

We thank Ms M. Asakawa and M. Kurita for their excellent assistance. This work was partly supported by a Research Grant from the Ministry of Health, Labour and Welfare (Japan), and a Grant-in-Aid for Scientific Research from the Ministry of Education, Culture, Sports, Science and Technology (Japan).

References

Akopian A. N., Okuse K., Souslova V., England S., Ogata N. and Wood J. N. (1999) *Trans*-splicing of voltage-gated sodium channel is regulated by nerve growth factor. *FEBS Lett.* **445**, 177–182.

Carmichael G. G. (2003) Antisense making more sense. *Nat. Biotechnol.* **21**, 371–372.

Caudevilla C., Serra D., Miliar A., Codony C., Asins G., Bach M. and Hegardt F. (1998) Natural *trans*-splicing in carnitine octanoyltransferase pre-mRNAs in rat liver. *Proc. Natl Acad. Sci. USA* **95**, 12 185–12 190.

Chomczynski P. and Sacchi N. (1987) Single-step method of RNA isolation by acid guanidinium thiocyanate–phenol–chloroform extraction. *Anal. Biochem.* **162**, 156–159.

Dannysz W. and Parsons A. C. (1998) Glycine and *N*-methyl-D-aspartate receptors: physiological significance and possible therapeutic applications. *Pharmacol. Rev.* **50**, 597–664.

Dunlop D. S. and Neidle A. (1997) The origin and turnover of D-serine in brain. *Biochem. Biophys. Res. Commun.* **235**, 26–30.

Foley K. P., Leonard M. W. and Engel J. D. (1993) Quantitation of RNA using the polymerase chain reaction. *Trends Genet.* **9**, 380–385.

Fujii N. (2002) D-Amino acids in living higher organisms. *Org. Life Evol. Biosph.* **32**, 103–127.

Fukasawa Y., Segawa H., Kim j. Y., Chairoungdua A., Kim D. K., Matsuo H., Cha S. H., Endou H. and Kanai Y. (2000) Identification and characterization of a Na^+-independent neutral amino acid transporter that associates with the 4F2 heavy chain and exhibits substrate selectivity for small neutral D- and L-amino acids. *J. Biol. Chem.* **275**, 9690–9698.

Hashimoto A., Nishikawa T., Hayashi T., Fujii N., Harada K., Oka T. and Takahashi K. (1992) The presence of free D-serine in rat brain. *FEBS Lett.* **296**, 33–36.

Hashimoto A., Kumashiro S., Nishikawa T. *et al.* (1993a) Embryonic development and postnatal changes in free D-aspartate and D-serine in the human prefrontal cortex. *J. Neurochem.* **61**, 348–351.

Hashimoto A., Nishikawa T., Konno R., Niwa A., Yasumura Y., Oka T. and Takahashi K. (1993b) Free D-serine, D-aspartate and D-alanine in central nervous system and serum in mutant mice lacking D-amino acid oxidase. *Neurosci. Lett.* **152**, 33–36.

Hashimoto A., Nishikawa T., Oka T. and Takahashi K. (1993c) Endogenous D-serine in rat brain: *N*-methyl-D-aspartate receptor-related distribution and aging. *J. Neurochem.* **60**, 783–786.

Hashimoto A., Oka T. and Nishikawa T. (1995a) Extracellular concentration of endogenous free D-serine in the rat brain as revealed by *in vivo* microdialysis. *Neuroscience* **66**, 635–643.

Hashimoto A., Oka T. and Nishikawa T. (1995b) Anatomical distribution and postnatal changes in endogenous free D-aspartate and D-serine in rat brain and periphery. *Eur. J. Neurosci.* **7**, 1657–1663.

Hashimoto T., Kajii Y. and Nishikawa T. (1998) Psychotomimetic-induction of tissue plasminogen activator mRNA in corticostriatal neurons in rat brain. *Eur. J. Neurosci.* **10**, 3387–3399.

Hayashi F., Takahashi K. and Nishikawa T. (1997) Uptake of D- and L-serine in C6 glioma cells. *Neurosci. Lett.* **239**, 85–88.

Horiike K., Tojo H., Arai R., Nozaki M. and Maeda T. (1994) D-Amino-acid oxidase is confined to the lower brain stem and cerebellum in rat brain: regional differentiation of astrocytes. *Brain Res.* **652**, 297–303.

Javitt D. C. (2004) Glutamate receptors as therapeutic targets. *Mol. Psychiatry* **9**, 979.

Javitt D. C., Balla A. and Sershen H. (2002) A novel alanine-insensitive D-serine transporter in rat brain synaptosomal membranes. *Brain Res.* **941**, 146–149.

Kajii Y., Muraoka S., Hiraoka S., Fujiyama K., Umino A. and Nishikawa T. (2003) A developmentally regulated and psychostimulant-inducible novel rat gene *mrt1* encoding PDZ-PX proteins isolated in the neocortex. *Mol. Psychiatry* **8**, 434–444.

Kattenstroth G., Tantalaki E., Südhof T. C., Gottmann K. and Missler M. (2004) Postsynaptic *N*-methyl-D-aspartate receptor function requires α-neurexins. *Proc. Natl Acad. Sci. USA* **101**, 2607–2612.

Korneev S. and O'Shera M. (2002) Evolution of nitric oxide synthase regulatory genes by DNA inversion. *Mol. Biol. Evol.* **19**, 1228–1233.

Korneev S. A., Park J. and O'Shea M. (1999) Neuronal expression of neural nitric oxide synthase (nNOS) protein is suppressed by antisense RNA transcribed from NOS pseudogene. *J. Neurosci.* **19**, 7711–7720.

Lefauconnier J. M. and Trouve R. (1983) Developmental changes in the pattern of amino acid transport at the blood–brain barrier in rats. *Brain Res.* **282**, 175–182.

Lehner B., Williams G., Campbell R. D. and Sanderson C. M. (2002) Antisense transcripts in the human genome. *Trends Genet.* **18**, 63–65.

Lombardo J. and Brown G. B. (1996) A quantitative and specific method for measuring transcript levels of highly homologous genes. *Nucl. Acids Res.* **24**, 4812–4816.

Missler M., Zhang W., Rohlmann A., Kattenstroth G., Hammer R. E., Gottmann K. and Südhof T. C. (2003) α-Neurexins couple Ca^{2+} channels to synaptic vesicle exocytosis. *Nature* **424**, 939–948.

Monyer H., Sprengel R., Schoepfer R., Herb A., Higuchi M., Lomeli H., Burnashev N., Sakmann B. and Seeburg P. H. (1992) Heteromeric NMDA receptors: molecular and functional distinction of subtypes. *Science* **256**, 1217–1221.

Nakanishi S. (1992) Molecular diversity of glutamate receptors and implications for brain function. *Science* **258**, 597–603.

Nishikawa T., Hashimoto A., Tanii Y., Umino A., Kashiwa A., Kumashiro S., Nihijima K., Oka T., Shirayama Y. and Takahashi K. (1994) Disturbed neurotransmission via the *N*-methyl-D-aspartate receptor and schizophrenia, in *The Biology of Schizophrenia* (Moroji T. and Yamamoto K., eds) pp. 197–207. Development of Psychiatry Series. Elsevier, Amsterdam.

Ogawa M., Shigeto H., Yamamoto T., Oya Y., Wada K., Nishikawa T. and Kawai M. (2003) D-Cycloserine for the treatment of ataxia in spinocerebellar degeneration. *J. Neurol. Sci.* **210**, 53–56.

Osoegawa K., Tateno M., Woon P. Y., Frengen E., Mammoser A. G., Catanese J. J., Hayashizaki Y. and de Jong P. (2000) Bacterial artificial chromosome libraries for mouse sequencing and functional analysis. *Genome Res.* **10**, 116–128.

Pirrotta V. (2002) Trans-*splicing in* Drosophila. *Bioessays* **24**, 988–991.

Ribeiro C. S., Reis M., Panizzutti R., de Miranda J. and Wolosker H. (2002) Glial transport of the neuromodulator D-serine. *Brain Res.* **929**, 202–209.

Schell M. J., Molliver M. E. and Snyder S. H. (1995) D-Serine, an endogenous synaptic modulator: localization to astrocytes and glutamate-stimulated release. *Proc. Natl Acad. Sci. USA* **92**, 3948–3952.

Schell M. J., Brady R. O., JrMolliver M. E. and Snyder S. H. (1997) D-Serine as a neuromodulator: regional and developmental localizations in rat brain glia resemble NMDA receptor. *J. Neurosci.* **17**, 1604–1615.

Takahara T., Kasahara D., Mori D., Yanagisawa S. and Akanuma H. (2002) The *trans*-spliced variants of Sp1 mRNA in rat. *Biochem. Biophys. Res. Commun.* **298**, 156–162.

Takahashi K., Hayashi F. and Nishikawa T. (1997) *In vivo* evidence for the link between L- and D-serine metabolism in rat cerebral cortex. *J. Neurochem.* **69**, 1286–1290.

Toda S., Kajii Y., Sato M. and Nishikawa T. (2000) Reciprocal expression of infant- and adult-preferring transcripts of CDCrel-1 septin gene in the rat neocortex. *Biochem. Biophys. Res. Commun.* **273**, 723–728.

Tsuchida H., Yamamoto N., Kajii Y., Umino A., Fukui K. and Nishikawa T. (2001) Cloning of a D-serine-regulated transcript *dsr-1* from the rat cerebral cortex. *Biochem. Biophys. Res. Commun.* **280**, 1189–1196.

Urai Y., Jinnouchi O., Kwak K. T., Suzue A., Nagashiro S. and Fukui K. (2002) Gene expression of D-amino acid oxidase in cultured rat astrocytes: regional and cell type specific expression. *Neurosci. Lett.* **324**, 101–104.

Ushkaryov Y. A. and Südhof T. C. (1993) Neurexin IIIα: extensive alternative splicing generates membrane-bound and soluble forms. *Proc. Natl Acad. Sci. USA* **90**, 6410–6414.

Vanhée-Brossollet A. and Vaquero C. (1998) Do natural antisense transcripts make sense in eukaryotes? *Gene* **211**, 1–9.

Wako K., Ma N., Shiroyama T. and Semba R. (1995) Glial uptake of intracerebroventriculaly injected D-serine in the rat brain: an immunocytochemical study. *Neurosci. Lett.* **185**, 171–174.

Watanabe M., Inoue Y., Sakimura K. and Mishina M. (1992) Developmental changes in distribution of NMDA receptor channel subunit mRNAs. *Neuroreport* **3**, 1138–1140.

Welsh J., Chada K., Dalal S. S., Cheng R., Ralph D. and McClelland M. (1992) Arbitrarily primed PCR fingerprinting of RNA. *Nucl. Acids Res.* **20**, 4965–4970.

Wolosker H., Blackshaw S. and Snyder H. (1999) Serine racemase: a glial enzyme synthesizing D-serine to regulate glutamate-*N*-methyl-D-aspartate neurotransmission. *Proc. Natl Acad. Sci. USA* **96**, 13 409–13 414.

Woon P. Y., Osoegawa K., Kaisaki P. J. *et al.* (1998) Construction and characterization of a 10-fold genome equivalent rat P1-derived artificial chromosome library. *Genomics* **50**, 306–316.

Yamamoto N., Tomita U. and Umino A. and. Nishikawa T. (2001) Uptake of D-serine by synaptosomal P2 fraction isolated from rat brain. *Synapse* **42**, 84–86.

Yang Y., Ge W., Chen Y., Zhang Z., Shew W., Wu C., Poo M. and Duan S. (2003) Contribution of astrocytes to hippocampal long-term potentiation through release of D-serine. *Proc. Natl Acad. Sci. USA* **100**, 15 194–15 199.

Current Topics

D-Amino Acid Biosystem

Metabolism and Functional Roles of Endogenous D-Serine in Mammalian Brains

Toru NISHIKAWA

Section of Psychiatry and Behavioral Sciences, Tokyo Medical and Dental University Graduate School; Bunkyo-ku, Tokyo 113–8519, Japan.

Received May 9, 2005

It has now been well established that D-serine, a coagonist for the *N*-methyl-D-aspartate (NMDA) glutamate receptors (NR1/NR2 type), is maintained at a high concentration in mammalian brains for life and shows a brain-selective and NMDA receptor R2B subunit-related distribution, overturning the hitherto generally accepted theory that D-amino acid is not always present in mammalian tissues. D-Serine in the brain has been shown to be contained in both the glia and neurons and to have specific processes of biosynthesis, extracellular release, uptake, and degradation. Moreover, the selective elimination of D-serine reduces the NMDA receptor-mediated intracellular signaling and long-term potentiation of synaptic connections. Together with the anti-psychotic and anti-ataxic property of D-serine and the pivotal roles of the NMDA receptor in divergent higher brain functions, these observations support the view that the D-amino acid may be involved as an endogenous modulator for the NMDA receptor in various neuropsychiatric functions and their pathological conditions.

Key words brain; neuropsychiatric disorder; *N*-methyl-D-aspartate (NMDA) glutamate receptor; D-serine

The discovery of endogenous D-serine in the mammalian brain between 1990 and 1991 by the present author with my collaborators at the National Institute of Neuroscience, NCNP, in Tokyo and other institutes, was a consequence of my research project on the pathophysiology and novel pharmacotherapy of schizophrenia using D-serine and D-alanine, which facilitate the *N*-methyl-D-aspartate (NMDA) glutamate receptor function *via* its glycine site (Fig. 1), by noting the induction of schizophrenia-like psychosis by the glutamate receptor antagonists such as phencyclidine (PCP).[1—5] According to this author's idea to overcome the low ability of these polar D-amino acids to cross through the blood brain barrier (BBB) that their apolar compounds could easily permeate the BBB and improve the schizophrenic symptoms by their systemic administration, Dr. Hibino at Nippon Oil and Fats, Co., Ltd., designed and synthesized for our experiments, *N*-myristoyl-D-serine and *N*-myristoyl-D-alanine, which were shown to ameliorate an animal model of schizophrenia, PCP-induced abnormal behavior, following their intraperitoneal injection.[3,6] During the process of the verification of the expected presence of free D-serine or D-alanine in the brain of animals treated with their fatty acid compounds by collaboration with the late Dr. Hayashi at the National Institute of Neuroscience and Dr. Fujii at Tsukuba University, we provided the first evidence that free D-serine is constantly maintained at a high concentration in the mammalian brain[7,8] although D-amino acids were believed to be uncommon in mammalian tissues based on previous studies.[9] Through immediate confirmations[10,11] of our findings, subsequent studies on endogenous D-serine have been gradually extended in a variety of aspects. In this article, the present status and future problems are discussed.

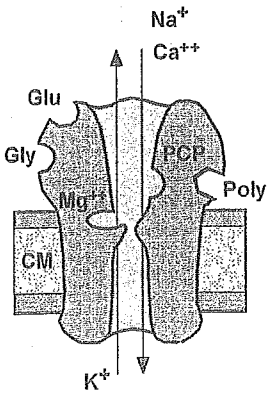

Fig. 1. Schematic Representation of the NMDA Receptor Ion Channel (NR1/NR2 Type)

The NMDA receptor complex has the multiple regulatory binding sites for glutamate (Glu), glycine and D-serine (Gly), magnesium ions (Mg^{++}), phencyclidine (PCP), and polyamine (Poly). This heteromeric receptor consists of an NR1 subunit (there are various variants) and at least one of 4 types of the NR2 subunits, A-D. Gly is considered to be present on NR1 and Glu on NR2. The more recently identified NR3 subunit could have regulatory sites that differ from those shown in this scheme.

1. DISTRIBUTION AND METABOLISM OF ENDOGENOUS D-SERINE IN THE MAMMALIAN BRAIN

1) Distribution In mature rats, D-serine is predominantly concentrated in the brain,[8] and its contents in the spinal cord, each peripheral tissue, or the blood are very low[8] (but high in the urine[12]). The D-serine distribution in the brain is also uneven, showing high concentrations in the forebrain areas including the cerebral cortex, hippocampus, striatum, and limbic forebrain, moderate to low concentrations in the diencephalon and midbrain, and trace levels in the pons-medulla and cerebellum.[8] The forebrain-preferred distribution of D-serine is positively correlated with those of the glutamate, PCP, and glycine sites of the NMDA receptor and particularly with that of the NMDA receptor R2B subunit mRNA.[8,13] These characteristics of the endogenous D-serine distribution have been ascertained by subsequent biochemical[11,14,15] and immunohistochemical studies using the anti-D-serine antibody,[16—18] and proved to be common to humans

e-mail: tnis.psyc@tmd.ac.jp

and other mammalians.[11,14,19,20] At the cell level,[16—18] a D-serine-like immunoreactivity has been described in astrocytes, oligodendrocytes and the cell bodies, dendrites, and axons of neurons.

The D-serine distribution in the brain significantly changes with postnatal development,[8,14,15,21] and is almost homogenous immediately after birth but approaches the pattern of the mature stage during the 3-week period after birth in the rat.[8,14,21] These developmental changes are also similar to those for the distribution of the R2B subunit mRNA in the brain.[8, 13,14,21]

2) Extracellular Release D-Serine is detected in extracellular fluid by an *in vivo* dialysis technique in the medial frontal cortex, striatum and cerebellum.[22] The extracellular contents of D-serine are closely correlated with its concentration in tissue (about 5×10^{-6} M in the cortex of the medial frontal cortex) and the NMDA receptor distribution.[22] Unlike classical neurotransmitters, such as glutamate, glycine and dopamine, the amount of D-serine in the frontal extracellular fluid was not increased, but rather decreased, by depolarization following a veratrine or high concentration of potassium ion application.[22] Furthermore, the interruption of the nerve impulse flow or removal of extracellular calcium ions failed to reduce the extracellular D-serine levels.[22]

In vitro studies using cultured astrocytes from the rat cerebral cortex or C6 glioma cells[16,23] indicate that kainite- and AMPA ((S)-α-amino3-hydroxy-5-methyl-4-isoxazolepropionic acid) induce the D-serine release. In contrast to the spontaneous liberation, this evoked release is shown to be dependent upon the calcium ion and SNARE (soluble *N*-ethylmaleimide-sensitive factor attachment protein receptor) protein as other transmitters released from the astroglial cells including glutamate and ATP.[23] The relationship between the evoked and the basal (spontaneous) release of D-serine awaits further elucidation.

3) Uptake Rat brain homogenates[24—26] and C6 cells[27] have been demonstrated to have a sodium-dependent or -independent, saturable and temperature-sensitive uptake activity for D-serine. The pharmacological characteristics of the D-serine uptake by rat brain homogenates differ from those of the uptake of known transporters. Although a specific and physiological transporter for D-serine has not yet been identified, it is of interest to note that the sodium-independent neutral amino acid transporter Asc1 shows a high affinity not only to L-serine, L-cysteine, and L-alanine, but also to D-serine.[28]

4) Synthesis In the rat brain, the augmented concentration of L-serine by its systemic administration results in an increase in the D-serine content, and *vise versa*.[29] Moreover, [^{3}H]L-serine has been shown to be converted into [^{3}H]D-serine.[30] These phenomena suggest the presence of a serine racemase that catalyzes the synthesis of D-serine from L-serine. Indeed, a pyridoxal 5′-phosphate-dependent serine racemase with D- and L-serine α,β-elimination activities has been reported in rat and human tissues.[31,32] However, it cannot be excluded that D-serine biosynthesis might be regulated by other enzymes, such as a phosphoserine phosphatase, glycine cleavage system and serine hydroxymethyl transferase, because of 1) the formation of D-serine from L-phosphoserine in brain synaptosomes,[33] 2) a reduction in the D-serine contents in the cerebral cortex of patients with non-ketotic hyperglycinemia lacking the glycine cleavage system and of the rat treated with an inhibitor of this enzyme system,[34] and 3) an increase in the brain D-serine concentrations by application of glycine.[29]

5) Degradation A long-known mammalian enzyme, D-amino acid oxidase (DAO), has a D-serine degradation activity.[35,36] In the rat brain, the distribution and its postnatal development of DAO are inversely correlated with those of D-serine; the DAO activity rapidly increases in the cerebellum, pons, and medulla oblongata about 10 d after birth,[36,37] when the D-serine concentration begins to decrease.[14,21] In mutant mice lacking this enzyme activity, there is a marked and very slight increase in D-serine contents in the cerebellum and cerebral cortex, respectively.[37] These findings indicate the involvement of DAO in the formation of a D-serine concentration gradient in the brain, and, at least, in the D-serine degradation in the metencephalon. A very slight activity,[37] mRNA expression[39] and immunoreactivity[16,37] of DAO in the forebrain tissues or astrocytes cultured from the rat cerebral cortex do not deny the possible presence of other enzymes that catalyze the physiological D-serine degradation in the forebrain areas.

6) D-Serine Responsive Novel Genes We have recently isolated two novel transcripts, dsr-1 (D-serine-responsive transcript-1)[40] and dsr-2,[41] of which the expressions are selectively induced by D-serine but not by L-serine. A part of dsr-1 is homologous with the M9.2 gene that encodes the proton ATPase subunit, suggesting its possible involvement in the D-serine uptake and release.[40] Also, dsr-2 seems to be involved in the metabolism or functions of D-serine, because the mRNAs of dsr-2 are exclusively expressed in the brain and show a D-serine- and NMDA receptor R2B subunit-like distribution in the brain.[41]

2. PHYSIOLOGICAL FUNCTIONS OF D-SERINE IN THE BRAIN

1) Regulation of the NMDA Receptor i) NMDA Receptors Consisting of NR1 and NR2 Subunits (Fig. 1): Before D-serine was found to be an endogenous substance, this D-amino acid was initially known as a selective agonist for the glycine-binding site of the NMDA receptor.[42] Like glycine and D-alanine, D-serine stimulates the glycine site of the NMDA type receptor consisting of NR1 and NR2 subunits and enhances the action of glutamate on the receptor as follows[42]: (a) depolarization, (b) inward electric current, (c) Ca^{++} inflow, (d) cGMP production, (e) release of various neurotransmitters, and (f) neuron death. Stimulation of the glycine modulatory site alone does not induce excitatory postsynaptic potentials, but is indispensable for adequate neurotransmission by glutamate.[42] Consequently, glycine, D-serine, and D-alanine are called "co-agonists" for the NMDA receptor.[42] The actions of the two D-amino acids are stereoselective and much more potent than the respective L-amino acids.[42]

Together with these characteristic actions, the NMDA receptor-like distribution of D-serine in the mammalian brains (see 1.-1)) suggests that D-serine in the brain is a physiological co-agonist for the NMDA receptor.[8] Glycine is another intrinsic co-agonist of the NMDA receptor with a different distribution pattern and metabolic pathway in the brain from

Table 1. Comparison between D-Serine and Glycine as the Endogenous Ligands for the Glycine Modulatory Site of the NMDA Receptor (NR) in Mammalian Brains

	D-Serine	Glycine
Binding selectivity		
NR-associated glycine site	High affinity	High affinity
Inhibitory glycine receptor	Low affinity	High affinity
Effects on NR1/NR2 receptor	Facilitatory	Facilitatory
Effects on NR1/NR3 receptor	Inhibitory	Excitatory[a]
Distribution: Adult period	Brain-selective	Ubiquitous in CNS & periphery
	Forebrain-dominant	Hindbrain-preferential
	NR2B-related	NR-unrelated?
Postnatal development	NR2B-related	NR-unrelated?
Immunoreactivity	Neuron<Glia	Neuron>Glia
Precursor	L-Serine and/or glycine?	L-Serine
Synthesis	Serine racemase?	Serine hydroxymethyl transferase
Extracellular release	Depolarization-induced increase (−)	Depolarization-induced increase (+)
Uptake	(+): Na-dependent & -independent	(+): Na-dependent
Transporter	? (asc1?)	GLYT1 & GLYT2
Degradation	D-Amino acid oxidase?	Glycine cleavage system
Effects of depletion on NR	NR hypofunction	?
Roles in neurotransmission	Neuromodulator	Inhibitory transmitter[a]/Neuromodulator

CNS, central nervous system; NR, NMDA receptor; NR-associated glycine site, strychnine-insensitive glycine receptor (cf. inhibitory glycine receptor, strychnine-sensitive glycine receptor). *a*) Note that glycine alone has been reported to induce the excitatory responses in the NR1/NR3 type heteromeric NR receptor.

D-serine and/or the NMDA receptor[8] (Table 1). The neurobiological differences indicate the distinct physiological roles between D-serine and glycine in the control of the NMDA receptor, which are still unclear (Table 1).

The pivotal role of D-serine in the NMDA receptor activation is supported by the fact that in the hippocampal slice preparation, selective depletion of the endogenous D-serine in the hippocampal slice preparation by DAO results in a marked inhibition of the NMDA receptor-mediated spontaneous and evoked synaptic currents,[43] nitric oxide synthase activation,[43] cGMP production[43] and long-time potentiation (LTP) induction[44] without significant changes in the glycine contents. The 4 types of heteromeric NMDA receptors in any combination with NR2A-NR2D and NR1 that are expressed on the Xenopus oocytes displayed no differences in responses to D-serine and glycine.[45] The enhancing effect of D-serine on the glutamate-induced inward current was several times as potent as that of glycine in each type of receptor.[45]

ii) NMDA Receptors Composed of NR1 and NR3 Subunits: Heteromeric NMDA receptors composed of NR1 and NR3A or NR3B respond to neither glutamate nor NMDA, but glycine induces excitatory responses (inward current).[46] Interestingly, D-serine shows an action opposite to that of glycine in the NR1/NR3 NMDA receptors, having negligible effects when used alone, but markedly blocking the glycine-induced inward currents.[46] Therefore, D-serine is also a candidate as an endogenous modulator for NR1/NR3 type NMDA receptors, but not a co-agonist.

2) Glia/Neuron Interaction The lack of increase in the levels of the extracellular D-serine following depolarization stimuli[23] and a substantial D-serine-like immunoreactivity in the glia cells including astrocytes[16,18] suggest that D-serine may be released as a neuromodulator from these glia cells. Several studies indeed reported the presence of a serine racemase-like immunoreactivity,[23,31] uptake[16] and release[16,23] activity of D-serine and DAO mRNA[39] in the astrocyte. The D-serine synthesis in the astrocytes is also indicated to depend on the co-existence of neurons in the culture system.[44] These observations are consistent with the idea that D-serine may be implicated in the glia-neuron interaction that is required for the control of the NMDA receptor in the brain, although its exact cellular setups remain to be clarified.

3) Neural Circuit Formation In the cerebellar slices, D-serine is shown to enhance granule cell migration while the selective degradation of D-serine by DAO and pharmacologic attenuation of the serine racemase activity hamper the process.[47] These phenomena suggest the involvement of brain D-serine in neural circuit formation possibly *via* the NMDA receptors in a certain growth stage or during repair of the nerve wiring.

3. D-SERINE AND NEUROPSYCHIATRIC DISORDERS

1) Implications for the Pathophysiology D-Serine, a putative endogenous co-agonist for the NR1/NR2 type NMDA receptor, is supposed to play a critical role in the development and control of various higher brain functions in which NMDA receptors are involved. Therefore, disturbances in the brain D-serine and the molecular system for its metabolism and function may induce a variety of neuropsychiatric symptoms. Indeed, substances including D-serine that act on the glycine site of the NMDA receptor influence schizophrenic symptoms[48] and their animal models,[1—5,49] cerebral ataxia,[50,51] the action of alcohol,[42] learning ability in dementia model animals,[42] anxiety behavior,[42] convulsion threshold,[42] ischemic neuron death,[42,52] and long-term behavioral abnormalities due to drug dependence.[42] A drastic reduction in the brain D-serine contents was found in patients with non-ketotic hyperglycinemia[34] lacking the glycine cleavage system who presented various central nervous symptoms such as mental retardation, convulsive attacks, apnea, and drowsiness. Particularly, attention has recently been directed to the possible association of endogenous D-serine with the pathophysiology of schizophrenia.

NMDA receptor antagonists acting at the PCP and glutamate site induce schizophrenia-like psychosis exhibiting both

positive (*e.g.*, hallucination and delusion) and negative (*e.g.*, affective flattening, alogia and avolition) symptoms in proportion to the potency of the blocking action.[1,48] In contrast, various symptoms in patients with schizophrenia have been demonstrated to be improved by the oral administration of glycine, D-cycloserine, or D-serine which facilitate the NMDA receptor function by stimulating the glycine modulatory site of the glutamate receptor.[48] Based on these observations, it is widely accepted that glutamate neurotransmission *via* the NMDA receptor may be decreased in schizophrenia.[48]

One possible cause of this decrease is the reduced activation of this receptor due to a deficit in the D-serine signals conveyed to the glycine site resulting from abnormalities in molecules crucial for the metabolism or function of the brain D-serine, although no direct evidence for this hypothesis has been so far provided. There are no reports describing significant changes in the D-serine concentrations in the postmortem brain tissues from the patients with schizophrenia as compared to those without neuropsychiatric disorders.[11,20] However, in the postmortem schizophrenic brains, an increase in the NMDA glycine binding sites was observed in some cerebral cortical areas,[54] which might be compensatory responses to the decreased extracellular D-serine release in the specific neural circuit. In addition, the association of single-nucleotide polymorphism markers from both the DAO gene and a new gene G72 from chromosome 13q34 with schizophrenia, together with an *in vitro* augmentation of DAO activity by a G72 protein product,[55] suggest an altered D-serine metabolism in this disorder.

2) Implications for the Development of Novel Pharmacotherapy Clinical studies have been performed to apply the anti-psychotomimetic[1,—5,49,55] and anti-ataxic[50,51] actions of D-serine or other agonists for the NMDA glycine site, which are proven in animal experiments, to the treatment of schizophrenia and cerebellar ataxia. As expected by the ability of NMDA antagonists to induce schizophrenia-like antipsychotic-insensitive symptoms, the glycine agonists including glycine, D-cycloserine, D-serine and a glycine transporter inhibitor, *N*-methylglycine, have been found to ameliorate the schizophrenic symptoms that are resistant to conventional pharmacotherapy.[48] We reported that a NMDA glycine site agonist, D-cycloserine, improved some ataxic movements in patients with spinocerebellar degeneration[50] for which there are few effective treatment drugs. The above clinically applicable NMDA receptor potentiators, however, have problems in the effective administration doses[48] and side effects.[56] Advances in the research on molecular mechanisms of the D-serine metabolism in the brain may allow a search for D-serine signal regulatory drugs targeting D-serine-associated molecules, such as D-serine-specific transporter inhibitors, and also overcome these problems.

4. CONCLUSION

Compelling evidence has been accumulated indicating that brain D-serine is a neuromodulator for, at least, the NMDA type glutamate receptor (Table 1) and is involved in a neuron-glia interaction, wiring and rearrangement of neuron circuits and behavioral expression in mammals. The NMDA co-agonist nature of D-serine suggests that the endogenous D-amino acid should be maintained above a certain concentration in synaptic clefts for the physiological glutamate transmission *via* the NMDA receptor and requires a distinct molecular and cellular system from those for classical neurotransmitters that should be rapidly removed after their quantal release in the synaptic clefts. This hypothesis appears to be consistent with the data showing the unique profiles of release, uptake and disappearance of D-serine in the brain tissues which are not seen in the other known neuroactive substances. Therefore, clarifying the molecular mechanisms of the metabolism and physiological function of the brain D-serine is expected to lead to not only new physiochemical findings, but also clues to unknown information processing systems controlling the brain functions, which may markedly promote the understanding of the cause/pathology of neuropsychiatric disorders and the development of new treatment methods.

Acknowledgments The author thank all my past and current collaborators concerned with the studies of D-serine described in this review article, who are listed as the co-authors of our papers in the reference section.

REFERENCES

1) Nishikawa T., Umino A., Tanii Y., Hashimoto A., Hata N., Takashima M., Takahashi K., Toru M., "Biological Basis of Schizophrenic Disorders," ed. by Nakazawa T., Japan Scientific Societies Press, Tokyo, 1991, pp. 65—76.
2) Tanii Y., Nishikawa T., Umino A., Takahashi K., *Neurosci. Lett.*, **112**, 318—323 (1990).
3) Tanii Y., Nishikawa T., Hashimoto A., Hibino H., Takahashi K., *Jpn. J. Psychiatry Neurl.*, **44**, 790 (1990).
4) Tanii Y., Nishikawa T., Hashimoto A., Takahashi K., *Brain Res.*, **563**, 281—284 (1991).
5) Tanii Y., Nishikawa T., Hashimoto A., Takahashi K., *J. Pharmacol. Exp. Ther.*, **269**, 1040—1048 (1994).
6) Tanii Y., Nishikawa T., Hashimoto A., Hibino H., Takahashi K., *Brain Science and Mental Disorders*, **2**, 497—502 (1991) (in Japanese with English abstract).
7) Hashimoto A., Nishikawa T., Hayashi T., Fujii N., Harada K., Oka T., Takahashi K., *FEBS. Lett.*, **296**, 33—36 (1992).
8) Hashimoto A., Nishikawa T., Oka T., Takahashi K. *J. Neurochem.*, **60**, 783—786 (1993).
9) Fujii N., *Orig. Life Evol. Biosph.*, **32**, 103—127 (2002).
10) Nagata Y., Yamamoto K., Shimojo T., Konno R., Yasumura Y., Akino T., *Biochim. Biophys. Acta*, **1115**, 208—211 (1992).
11) Chouinard M., Gaitan D., Wood P., *J. Neurochem.*, **61**, 1561—1564 (1993).
12) Bruckner H., Haasmann S., Friedrich A., *Amino Acids*, **6**, 205—211 (1994).
13) Watanabe M., Inoue Y., Sakimura K., Mishina M., *Neuroreport*, **3**, 1138—1140 (1992).
14) Nagata Y., Horiike K., Maeda T., *Brain Res.*, **634**, 291—295 (1994).
15) Hamase K., Homma H., Takigawa Y., Fukushima T., Santa T., Imai K., *Biochim. Biophys. Acta*, **1334**, 214—222 (1997).
16) Schell M. J., Molliver M. E., Snyder S. H., *Proc. Natl. Acad. Sci., U.S.A.*, **92**, 3948—3952 (1995).
17) Schell M. J., Brady R. O., Jr., Molliver M. E., Snyder S. H., *J. Neurosci.*, **17**, 1604—1615 (1997).
18) Yasuda E., Ma N., Semba R., *Neurosci. Lett.*, **299**, 162—164 (2001).
19) Hashimoto A., Kumashiro S., Nishikawa T., Oka T., Takahashi K., Mito T., Takashima S., Doi N., Mizutani Y., Yamazaki T., Kaneko T., Ootomo E., *J. Neurochem.*, **61**, 348—351 (1993).
20) Kumashiro S., Hashimoto A., Nishikawa T., *Brain Res.*, **681**, 117—125 (1995).
21) Hashimoto A., Oka T., Nishikawa T., *Eur. J. Neurosci.*, **7**, 1657—1663 (1995).

22) Hashimoto A., Oka T., Nishikawa T., *Neuroscience*, **66**, 635—643 (1995).
23) Mothet J. P., Pollegioni L., Ouanounou G., Martineau M., Fossier P., Baux G., *Proc. Natl. Acad. Sci., U.S.A.*, **102**, 5606—5611 (2005).
24) Yamamoto N., Tomita U., Umino A., Nishikawa T., *Synapse.*, **42**, 84—86 (2001).
25) Javitt D. C., Balla A., Sershen H., *Brain Res.*, **941**, 146—149 (2002).
26) Ribeiro C. S., Reis M., Panizzutti R., de Miranda J., Wolosker H., *Brain Res.*, **929**, 202—209 (2002).
27) Hayashi F., Takahashi K., Nishikawa T., *Neurosci. Lett.*, **239**, 85—88 (1997).
28) Fukasawa Y., Segawa H., Kim J. Y., Chairoungdua A., Kim D. K., Matsuo H., Cha S. H., Endou H., Kanai Y., *J. Biol. Chem.*, **275**, 9690—9698 (2000).
29) Takahashi K., Hayashi F., Nishikawa T., *J. Neurochem.*, **69**, 1286—1290 (1997).
30) Dunlop D. S., Neidle A., *Biochem. Biophys. Res. Commun.*, **235**, 26—30 (1997).
31) Wolosker H., Blackshaw S., Snyder S. H., *Proc. Natl. Acad. Sci., U.S.A.*, **96**, 13409—13414 (1999).
32) Foltyn V. N., Bendikov I., De Miranda J., Panizzutti R., Dumin E., Shleper M., Li P., Toney M. D., Kartvelishvily E., Wolosker H., *J. Biol. Chem.*, **280**, 1754—1763 (2005).
33) Wood P. L., Hawkinson J. E., Goodnough D. B., *J. Neurochem.*, **67**, 1485—1490 (1996).
34) Iwama H., Takahashi K., Kure S., Hayashi F., Narisawa K., Tada K., Mizoguchi M., Takashima S., Tomita U., Nishikawa T., *Biochem. Biophy. Res. Commun.*, **231**, 793—796 (1997).
35) Neims A. H., Zieverink W. D., Smilack J. D., *J. Neurochem.*, **13**, 163—168 (1966).
36) Weimar W. R., Neims A. H., *J. Neurochem.*, **29**, 649—656 (1977).
37) Horiike K., Tojo H., Arai R., Nozaki M., Maeda T., *Brain Res.*, **652**, 297—303 (1994).
38) Hashimoto A., Nishikawa T., Konno R., Niwa A., Yasumura Y., Oka T., Takahashi K., *Neurosci. Lett.*, **152**, 33—36 (1993).
39) Urai Y., Jinnouchi O., Kwak K. T., Suzue A., Nagahiro S., Fukui K., *Neurosci. Lett.*, **324**, 101—104 (2002).
40) Tsuchida H., Yamamoto N., Kajii Y., Umino A., Fukui K., Nishikawa T., *Biochem. Biophys. Res. Commun.*, **280**, 1189—1196 (2001).
41) Taniguchi G., Yamamoto N., Tsuchida H., Umino A., Shimazu D., Sakurai S., Takebayashi H., NishikawaT., *J. Neurochem.*, in press (2005).
42) Danysz W., Parsons A. C. G., *Pharmacol. Rev.*, **50**, 597—664 (1998).
43) Mothet J. P., Parent A. T., Wolosker H., Brady R. O., Linden D. J., Ferris C. D., Rogawski M. A., Snyder S. H., *Proc. Natl. Acad. Sci., U.S.A.*, **97**, 4926—4931 (2000).
44) Yang Y, Ge W., Chen Y., Zhang Z., Shen W., Wu C., Poo M., Duan S., *Proc. Natl. Acad. Sci., U.S.A.*, **100**, 15194—15199 (2003).
45) Matsui T., Sekiguchi M., Hasgimoto A., Tomita U., Nishikawa T., Wada K., *J. Neurochem.*, **65**, 454—458 (1995).
46) Chatterton J. E., Awobuluyi M., Premkumar L. S., Takahashi H., Talantova M., Shin Y., Cui J., Tu S., Sevarino K. A., Nakanishi N., Tong G., Lipton S. A., Zhang D., *Nature* (London), **415**, 793—798 (2002).
47) Kim P. M., Aizawa H., Kim P. S., Huang A. S., Wickramasinghe S. R., Kashani A. H., Barrow R. K., Huganir R. L., Ghosh A., Snyder S. H., *Proc. Natl. Acad. Sci., U.S.A.*, **102**, 2105—2110 (2005).
48) Javitt D. C., *Mol. Psychiatry*, **979**, 984—997 (2004).
49) Hashimoto A., Nishikawa T., Oka T., Takahashi K., *Eur. J. Pharmacol.*, **20**, 105—107 (1991).
50) Ogawa M., Shigeto H., Yamamoto T., Oya Y., Wada K., Nishikawa T., Kawai M., *J. Neurol. Sci.*, **210**, 53—56 (2003).
51) Saigoh K., Matsui K., Takahashi K., Nishikawa T., Wada K., *Brain Res.*, **808**, 42—47 (1998).
52) Katsuki H., Nonaka M., Shirakawa H., Kume T., Akaike A., *J. Pharmacol. Exp. Ther.*, **311**, 836—844 (2004).
53) Ishimaru M., Kurumaji A., Toru M., *Biol. Psychiatry*, **35**, 84—95 (1994).
54) Chumakov I., Blumenfeld M., Guerassimenko O., Cavarec L., Palicio M., Abderrahim H., Bougueleret L. P., Grel P., Debailleul V., Simon A. M., Caterina D., Dufaure I., Malekzadeh K., Belova M., Luan J. J., Bouillot M., Sambucy J. L., Primas G., Saumier M., Boubkiri N., Martin-Saumier S., Nasroune M., Peixoto H., Delaye A., Pinchot V., Bastucci M., Guillou S., Chevillon M., Sainz-Fuertes R., Meguenni S., Aurich-Costa J., Cherif D., Gimalac A., Van Duijn C., Gauvreau D., Ouellette G., Fortier I., Raelson J., Sherbatich T., Riazanskaia N., Rogaev E., Raeymaekers P., Aerssens J., Konings F., Luyten W., Macciardi F., Sham P. C., Straub R. E., Weinberger D. R., Cohen N., Cohen D., *Proc. Natl. Acad. Sci., U.S.A.*, **99**, 13675—13680 (2002).
55) Umino A., Takahashi K. Nishikawa T., *Br. J. Pharmacol.*, **124**, 377—385 (1998).
56) Carone F. A., Ganote C. E., *Arch. Pathol.*, **99**, 658—662 (1975).

Current Biology, Vol. 15, 587–593, March 29, 2005, ©2005 Elsevier Ltd All rights reserved. DOI 10.1016/j.cub.2005.01.058

The RNA Binding Protein TLS Is Translocated to Dendritic Spines by mGluR5 Activation and Regulates Spine Morphology

Ritsuko Fujii,[1,7] Shigeo Okabe,[2,4,7] Tomoe Urushido,[2] Kiyoshi Inoue,[1] Atsushi Yoshimura,[1] Taro Tachibana,[5] Toru Nishikawa,[3] Geoffrey G. Hicks,[6] and Toru Takumi[1,*]

[1]Osaka Bioscience Institute
Suita, Osaka 565-0874
Japan
[2]Department of Cell Biology
[3]Psychiatry and Behavioral Science
Tokyo Medical and Dental University Graduate School
Tokyo 113-8519
Japan
[4]Core Research for Evolutional Science and Technology
[5]Department of Applied and Bioapplied Chemistry
Graduate School of Engineering
Osaka City University
Osaka 558-8585
Japan
[6]Manitoba Institute of Cell Biology and University of Manitoba
Winnipeg, Manitoba R3E0V9
Canada

Summary

Neuronal dendrites, together with dendritic spines, exhibit enormously diverse structure [1]. Selective targeting and local translation of mRNAs in dendritic spines have been implicated in synapse remodeling or synaptic plasticity [2, 3]. The mechanism of mRNA transport to the postsynaptic site is a fundamental question in local dendritic translation [4, 5]. TLS (translocated in liposarcoma), previously identified as a component of hnRNP complexes, unexpectedly showed somatodendritic localization in mature hippocampal pyramidal neurons. In the present study, TLS was translocated to dendrites and was recruited to dendrites not only via microtubules but also via actin filaments. In mature hippocampal pyramidal neurons, TLS accumulated in the spines at excitatory postsynapses upon mGluR5 activation, which was accompanied by an increased RNA content in dendrites. Consistent with the in vitro studies, TLS-null hippocampal pyramidal neurons exhibited abnormal spine morphology and lower spine density. Our results indicate that TLS participates in mRNA sorting to the dendritic spines induced by mGluR5 activation and regulates spine morphology to stabilize the synaptic structure.

Results

TLS, also called FUS, was first identified as a rearranged gene at a chromosomal translocation junction invariably linked to human myxoid liposarcomas [6]. Recent structural study of TLS has identified 2-folded domains: a C4 zinc finger domain and RNA recognition motif (RRM) domain [7]. Consistent with its RNA binding properties, TLS is involved in rapid nuclear-cytoplasmic shuttling by binding mRNAs in the nucleus and exporting spliced mRNA as a ribonucleoprotein complex to the cytoplasm [8] and further in the initiation of cell spreading [9]. However, no neuronal function of TLS has been reported. Our initial observation that TLS is expressed in the mouse neocortex and hippocampus led us to investigate the neuronal functions of TLS.

TLS Localization in Mouse Neuronal Dendrites

TLS is expressed in the brain, and recent proteomic analysis revealed that TLS is included in an NMDA receptor complex [10] and an RNA-transporting granule as a binding partner of conventional kinesin (KIF5) [11]. We examined the subcellular distribution of TLS in hippocampal neurons in culture. Immunostaining with anti-TLS polyclonal antibody (TLS-C) exhibited a punctate distribution of TLS within dendrites and a clustering in the nucleus (Figure 1A, upper middle panel), whereas no specific signals were observed in the preadsorbed specimen (Figure 1A, upper right panel). Consistent with this endogenous expression of TLS, when expressed in the hippocampal neurons, TLS-fused to green fluorescent protein (TLS-GFP) exhibited a similar granular distribution within dendrites in addition to staining in the nucleus (Figure 1A, upper left panel). Furthermore, double-label immunocytochemistry with anti-TLS and anti-PSD95 antibodies revealed colocalization of TLS immunoreactivity with PSD95-positive spines (Figure 1A, arrows in lower panels) (the ratio of colocalization is 65%–73%, n = 50, dendritic segments from spiny neurons). This result suggests that TLS is localized in postsynapses and is consistent with further analysis described below (see Figure S1 in the Supplemental Data available with this article online). The hippocampal neurons expressing TLS-GFP were immunostained with anti-MAP2 antibody, a somatodendritic marker, to confirm that TLS was localized in the neuronal dendrites (Figure 1B, upper panels). The result clearly showed that TLS-GFP was colocalized with MAP2-immunopositive dendrites. In contrast, TLS-GFP was absent from long thin axonal projections of hippocampal pyramidal neurons marked by antibody against phosphorylated neurofilament protein (SMI31). The SMI31-positive projections were MAP2 negative, confirming their identity as axons (Figure 1B, lower panels). These results indicate that TLS is exclusively localized in the neuronal dendrites of polarized neurons.

TLS-GFP Moves toward Dendrites

TLS localization within dendrites was examined by using an adenovirus-mediated expression system to efficiently express TLS-GFP in cultured hippocampal neurons. Movement of TLS-GFP was assayed by time-lapse confocal microscopy 48 hr after infection with adenovirus expressing TLS-GFP (Figure 2 and Movies 1

*Correspondence: takumi@obi.or.jp
[7]These authors contributed equally to this work.

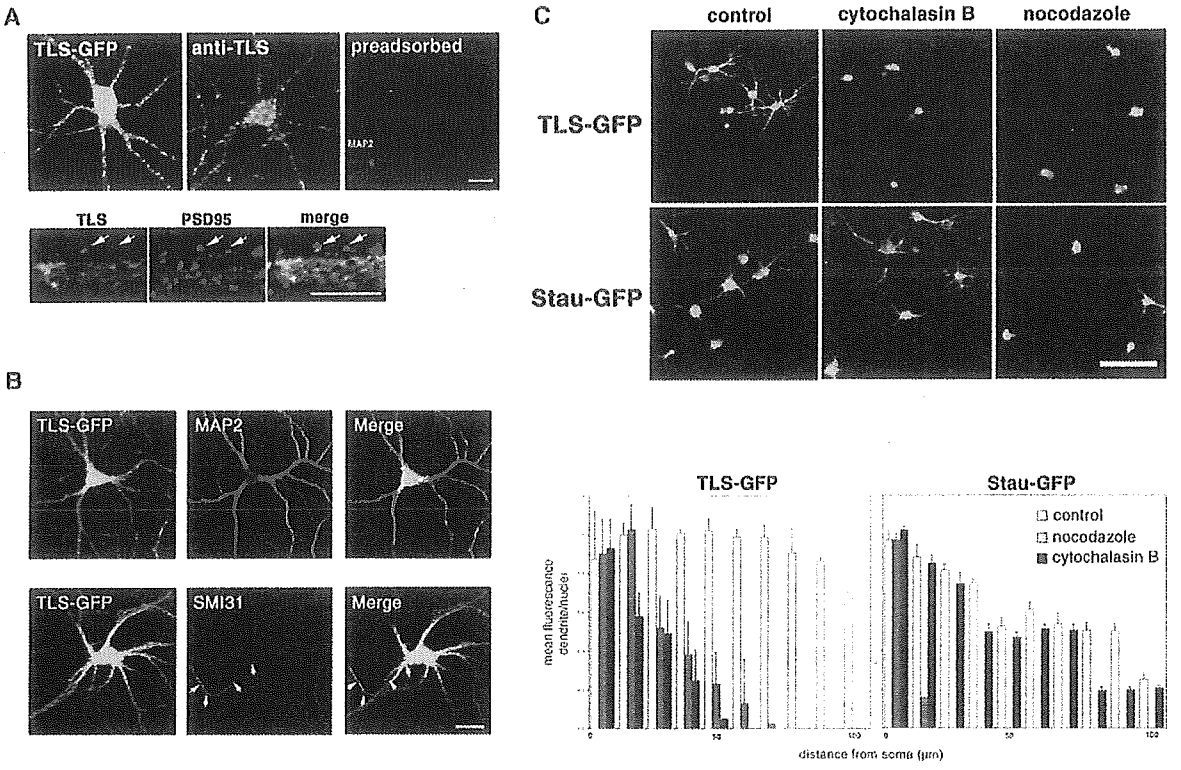

Figure 1. TLS Is Localized in Neuronal Dendrites

(A) Immunocytochemistry of mouse hippocampal-cultured neurons shows a punctate distribution of TLS within dendrites and its clustering in the nucleus (top middle). No staining with the antibody preadsorbed by excess amounts of GST-TLS fusion protein (top right, inset; costaining with anti-MAP2 antibody). Exogenously expressed TLS-GFP protein recapitulates the endogenous punctate localization of TLS within dendrites (top left). Double labeling with anti-PSD95 antibody shows that some of the TLS clusters are localized in spines (bottom arrows). Scale bars, 10 μm in upper panels and 5 μm in lower panels.

(B) TLS-GFP is localized in MAP2-positive neuronal dendrites, whereas TLS-GFP is absent in the MAP2-negative process (arrowheads). TLS-GFP is excluded from this SMI31-positive thin-axonal process (arrowheads) of a mouse hippocampal pyramidal neuron. Scale bars, 10 μm.

(C) TLS translocation to dendrites requires intact cytoskeletal polymers and is actin dependent. In control cells, TLS-GFP is distributed both in the cell bodies and dendrites (n = 27) as well as staufen-GFP. Treatment with either cytochalasin B (0.2 μM) (n = 48, over 50 μm distant from the soma, $p < 0.01$) or nocodazole (2 μM) (n = 51, over 70 μm distant from the soma, $p < 0.01$) for 12 hr reduces the amount of TLS-GFP within dendrites, although the neuronal extensions are not retracted. Nocodazole treatment blocks dendritic localization of staufen-GFP, however, cytochalasin B has no effect on its somatodendritic localization. Scale bar, 50 μm. Graphs showing quantitative data for pharamacological experiments with inhibitors described above are presented. Error bars indicate SEM (standard error of mean) for each experiment.

and 2). When TLS-GFP was expressed in immature dendrites with few spines (culture day 13, Figure 2A), rapid fusion (Figure 2A, 0–5 min, left arrows) and dissociation (Figure 2A, 0–5 min, right arrows) of a fraction of the TLS-GFP particles took place. Active movement of TLS-GFP particles over a short distance within dendrites was also observed (Figure 2A, 15–25 min, arrowhead). To measure the exchange rate of TLS-GFP molecules in the particles, we performed fluorescence recovery after photobleaching (FRAP) of TLS-GFP clusters present in dendrites. After photobleaching, fluorescent signals of TLS-GFP were recovered rapidly, and half recovery of fluorescence was observed within 20 s (data not shown). This rapid time course of FRAP recovery indicates a dynamic exchange of TLS molecules between particulate and soluble fractions. The movement of TLS-GFP was also revealed to be bidirectional, and some populations of TLS-GFP particles formed stationary clusters within the dendritic shaft (Figures S1Ba–S1Bc). These clusters also repeatedly gathered and dispersed within the dendrites. By double labeling with anti-cortactin binding protein (CortBP), as an independent marker that identifies the morphology of the spines, and TLS-GFP, we further analyzed whether TLS-GFP clusters are localized in spines (Figure S2). The distribution of spines/filopodia labeled with anti-CortBP was different from that of TLS-GFP clusters, indicating that TLS is not selectively translocated into spines/filopodia at the early developmental stage. In mature dendrites at culture day 23, there was a significant shift of the localization of TLS-GFP particles from the dendritic shafts to spines (Figure 2B, arrow; see also Figure S1A and S1Ca–S1Cc), and these particles within the spines did not show the rapid movement that was evident in the immature dendrites. TLS-GFP clusters within spines were of a stationary nature. These data suggest that TLS may move dynamically within dendrites before spine maturation. However, once im-

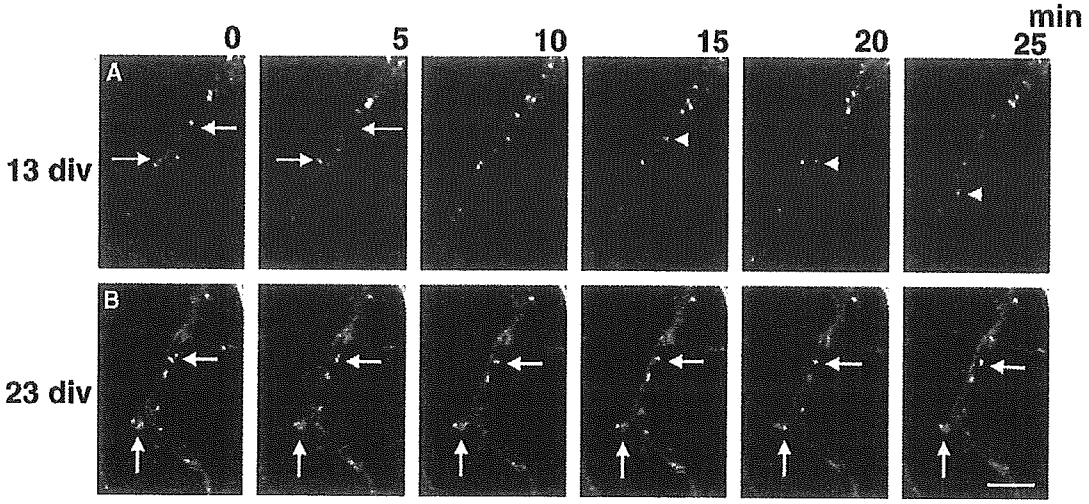

Figure 2. TLS-GFP Clusters Show Distinct Dynamics at Different Stages of Dendritic Maturation

TLS-GFP was expressed in mouse hippocampal neurons by use of the adenoviral expression system. TLS-GFP was assayed by time-lapse confocal imaging of TLS-GFP-expressing adenovirus 24–48 hr after the infection. (A) When TLS-GFP was expressed in immature dendrites with few spines (13 div: 13 days of in vitro culture), some TLS-GFP clusters fused together or dissociated during the short observation period of the time-lapse sequences (arrows in [A], 0–5 min). A fraction of TLS-GFP clusters actively moved a short distance in dendrites (arrowheads in [A], 15–25 min). (B) In mature dendrites (23 div: 23 days of in vitro culture), TLS-GFP clusters were stationary within spines and did not move as fast as they did in the immature dendrites. However, TLS-GFP clusters changed their shape actively, possibly because of the overall change of spine shape affected by actin-dependent motility (B, arrows). Scale bar, 5 μm.

mature spines are committed to form stable synapses, TLS may become preferentially recruited to and accumulated within spines.

Requirement of Intact Actin Polymers for TLS Translocation

To examine how the cytoskeletal organization of the dendrites is involved in the movement or transport of TLS, we treated primary cultured hippocampal neurons either with cytochalasin B or nocodazole, potent inhibitors of the assembly of actin filaments or microtubules, respectively. Both reagents affected the distribution of TLS within dendrites, and the TLS-GFP disappeared from the dendrites (Figure 1C). Quantitative analysis revealed a significant decrease in the TLS-GFP signal intensity in dendrites after treatment with either cytochalasin B or nocodazole (Figure 1C). On the other hand, the distribution of Staufen, whose dendritic localization is known to be microtubule dependent [12, 13], was affected by the nocodazole treatment, but not by cytochalasin B (Figure 1C). These data indicate that the dendritic localization of TLS-GFP required both actin filaments and microtubules.

Synaptic Activity-Dependent TLS Translocation to the Dendritic Spines

Mature dendrites expressing TLS-GFP were immunostained with anti-synapsin I antibody, anti-vesicular glutamate transporter-1 (VGLUT1) antibody, and anti-CortBP antibody to reveal the precise localization of TLS in dendrites. CortBP completely overlapped TLS-GFP at the synaptic sites (Figure S1F), whereas punctate structures immunopositive for either synapsin I, a marker of presynaptic vesicles, or VGLUT1, a marker of excitatory presynaptic structures, were closely apposed to the fluorescent clusters of TLS-GFP (Figure S1D and S1E, respectively), suggesting that TLS was specifically localized in the spines of excitatory postsynaptic sites, as described above.

Local protein synthesis subsequent to translocation of mRNA to dendrites is known to be stimulated by DHPG, a group 1 mGluR agonist [3], as well as neurotrophin, BDNF [14, 15]. Using DHPG to transiently activate mGluRs in dendrites, we tested to see if TLS-GFP accumulation in dendrites and dendritic spines depends on the state of synapse activation. When cultured hippocampal neurons expressing TLS-GFP were stimulated with DHPG (100 μM) over a 60-min period, the amount of TLS-GFP clusters in dendrites increased (Figures 3A–3D) and the movement of the particles accelerated (data not shown). Furthermore, the TLS-GFP clusters gradually accumulated in the dendritic spines (Figures 3A–3D, inset) where retrospective immunocytochemistry with synapsin I antibody revealed the presence of a presynaptic component at the sites of TLS accumulation (Figures 3D–3F). To the contrary, other synaptic proteins such as PSD95, Homer-1c (PSD-Zip45), Shank, and GKAP were not translocated into spines by DHPG treatment (see Figure S3). These results indicate that TLS is likely to be involved in the translocation of mRNA to the dendritic spines for local translation in dendrites. In DHPG-treated mature hippocampal neurons, the relative fluorescence intensity in spines was increased significantly (n = 26, cluster index 35% in average) by 5-fold compared with that of control neurons (n = 17, cluster index 7% in average) (Figure

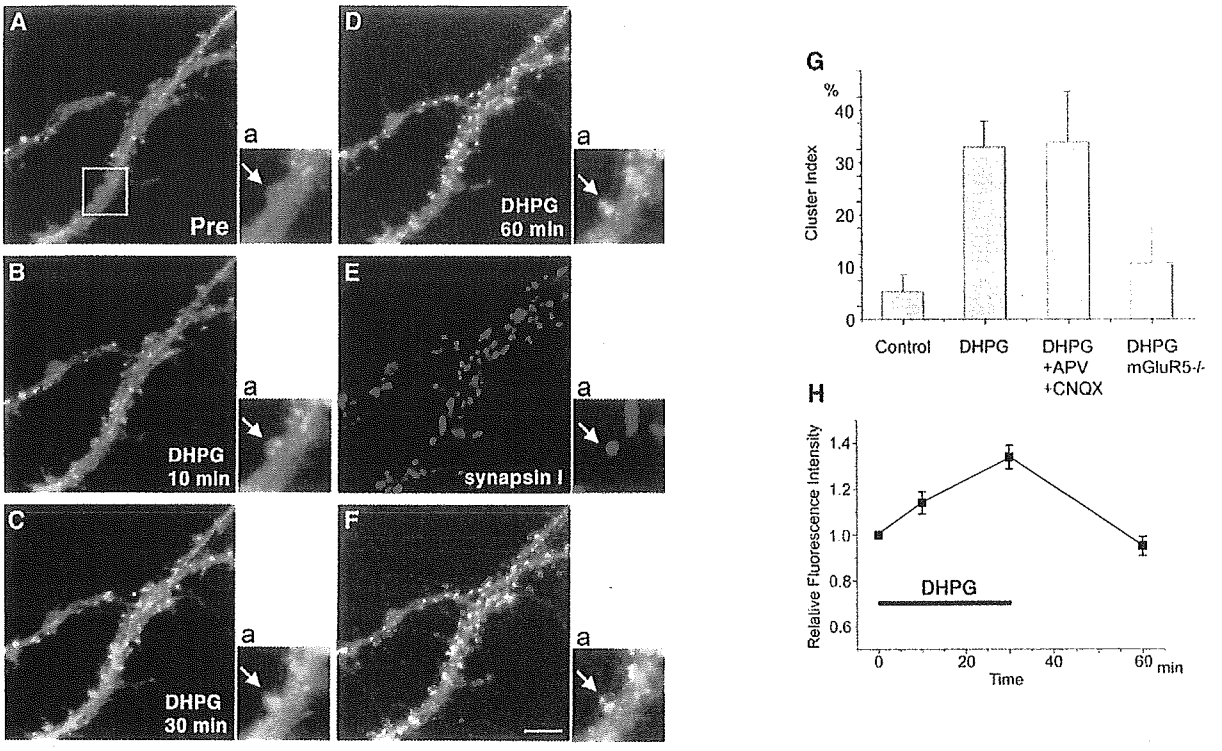

Figure 3. TLS Localization to the Postsynaptic Spines Is Dependent on mGluR Signals

(A–F) Time-lapse recording of TLS-GFP clusters after DHPG treatment (100 μM, 60 min) reveals that TLS-GFP accumulates within spines. (Aa–Fa) High-magnification view of the same area shown as a white rectangle in (A). Accumulation of TLS-GFP clusters takes place at the sites where retrospective immunocytochemistry by anti-synapsin I reveals the presence of presynaptic structures (E and F). Photos (F) and (Fa) are merged images of (D)–(E) and (Da)–(Ea), respectively.

(G and H) The average cluster index (the increase % of relative fluorescence intensity after the stimulation divided by the relative fluorescence intensity before the stimulation) is increased in cells treated with DHPG (n = 26). This DHPG-dependent effect does not change even in the combined presence of APV and CNQX (n = 7). The DHPG-dependent spine accumulation is abolished in hippocampal neurons from mGluR5$^{-/-}$ (n = 10). Control, n = 17 (H) DHPG (100 μM) induces accumulation of TLS-GFP in spines. However, upon the removal of DHPG 30 min after the start of treatment, the amount of TLS-GFP in spines returns to the control level. Error bars in (G) and (H) indicate SEM (n = 20).

3G). DHPG treatment did not change the number of the spines protruding from the shaft under the experimental conditions used nor caused significant elongation of the spines. Moreover, upon the removal of DHPG 30 min after the treatment, the number of spines containing TLS-GFP clusters moved back to the control level after another 30-min period of incubation (Figure 3H). This result clearly indicates that the spine localization induced by DHPG is a reversible event and that the spine localization was dependent on the state of mGluR activation. Hippocampal neurons expressing TLS-GFP were exposed to DHPG in the presence of both CNQX and APV, which are antagonists for the AMPA/kainate-type glutamate receptor (GluR) and NMDA receptor (NMDAR), respectively, to identify the signals responsible for the spine localization. The combination of CNQX and APV did not affect the DHPG-induced spine localization of TLS (Figure 3G), indicating that the spine localization was solely mediated by the mGluR activation and was independent of GluR or NMDAR activation. Because we demonstrated that TLS accumulated exclusively in the spines of postsynaptic neurons (Figure S1D–S1F), mGluR5, the major group 1 mGluR, was suspected to be the most plausible receptor candidate involved in TLS localization to the spines of pyramidal neurons in the CA1 area. To test this possibility, we examined the DHPG-induced TLS redistribution in hippocampal neurons derived from mGluR5 knockout mice [16]. In neurons of the mGluR5 homozygous mutants in which basal TLS distribution was not changed compared with wild-type (Figure S4), DHPG could not induce spine localization of TLS (Figure 3G). These results confirm that TLS accumulation in spines is induced upon postsynaptic activation of signaling cascades initiated by mGluR5.

Abnormal Spine Morphology in TLS-Deficient Mice

To investigate the context of TLS localization and its role in neuronal development, we prepared primary hippocampal neurons from embryos of TLS mutant mice (TLS$^{-/-}$) [17] and stained them with the lipophilic dye DiI (Figure 4). In the hippocampal neurons from the TLS-deficient mice, the dendrites were irregularly branched, and numerous long and thin processes like immature axons extended from the cell body (Figure 4A, arrows in upper panel of –/–), which is not observed in wild-type neurons extended with a single axon from the cell body (Figure 4A, arrows in upper panel of +/+). How-

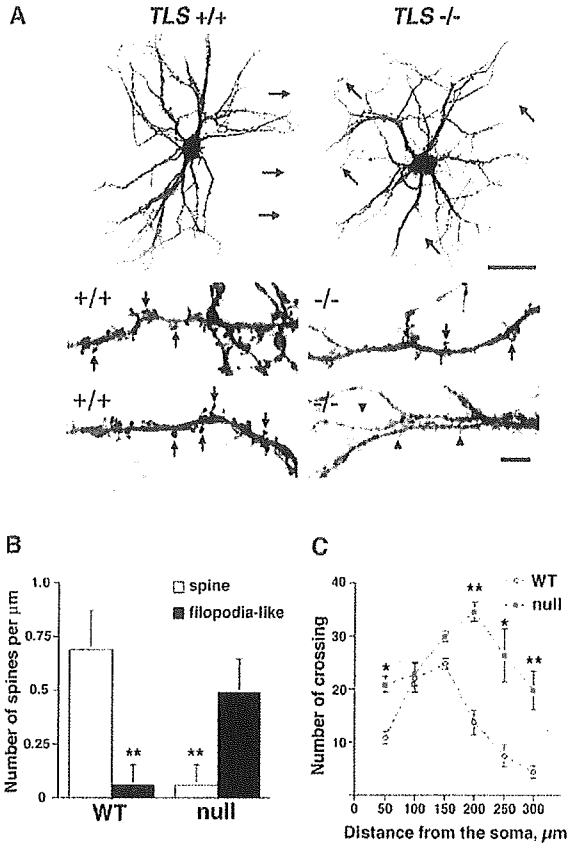

Figure 4. TLS-Deficient Mice Show Reduced Spine Number and Abnormal Spine Morphology

(A) Morphology of hippocampal neurons from TLS wild-type (*TLS*$^{+/+}$) and TLS null mutant (*TLS*$^{-/-}$) mice visualized by application of lipophilic dye DiI at 21 days in vitro. In neurons obtained from TLS$^{-/-}$ mice, there were multiple axon-like processes that have elongated from the soma (arrows in –/– of the upper panel). With higher magnification, the spines were reduced in their number (arrows in –/– of the middle panel) or transformed into thin cytoplasmic protrusion similar to filopodia (arrowheads in –/– of the lower panel). In contrast, majority of dendritic protrusions in wild-type neurons showed the morphology of mushroom-shaped spines, containing large heads connected to the shaft via thin neck (arrows in +/+ of the lower panels). Scale bars, 50 μm in upper panels and 5 μm in lower panels.

(B) Quantitative analysis of spine density in hippocampal neurons taken from wild-type (+/+) and TLS null mutant (–/–) mice. There was a significant decrease of spine density in the TLS null mice. On the other hand, the number of filopodia-like protrusions was significantly increased in TLS null neurons (50 representative dendrites from 10 neurons with each genotype were measured; double asterisk, $p < 0.01$). Error bars, SEM.

(C) Sholl profiles revealed a slight change in branching pattern of TLS null cultured pyramidal neurons. Number of dendritic crossings within 50 μm and over 200 μm from the soma significantly increased in TLS null neurons ($n = 30$ independent neurons). Asterisk, $p < 0.05$; double asterisk, $p < 0.01$.

ever, immunostaining for MAP2 or SMI31 revealed that TLS-null neurons possessed multiple dendrites and a single axon, indicating that the neuronal polarity was not affected by the TLS deficiency (data not shown). The spines in TLS-deficient neurons were reduced in number (Figure 4A, arrows in lower panel of –/–) or transformed into thin and long cytoplasmic protrusions similar to filopodia (Figure 4A, arrowheads in lower panel of –/–). Their structure was distinct from that of the wild-type hippocampal neuron spines, which displayed thin necks and relatively large heads and, thus, had a mushroom-like shape (Figure 4A, arrows in lower panel of +/+) [1]. Quantitative analysis revealed that the density of spines in TLS-deficient neurons was significantly reduced compared with that in the wild-type ones (Figure 4B). On one hand, the number of filopodia-like spines was increased in TLS-deficient neurons. To clarify further the difference in spine morphology between the TLS-deficient and wild-type neurons, we measured dendritic complexity by a standard Sholl analysis [18], which counts the number of dendritic crossings at 50 μm concentric circles. There were more branches in the proximal and distal region in TLS-deficient neurons compared with those in wild-type (Figure 4C). In the proximal region, more dendrites were elongated directly from the soma in the TLS null neurons. It appeared that there were more tertiary dendritic branches in the distal region of the TLS null neurons. These data imply a key role for TLS in neuronal maturation including dendritic branching and also maintenance of spine stability.

Discussion

Metabotropic glutamate receptors have diverse functions in signal transduction of neurons. Group 1 mGluRs, including mGluR1 and mGluR5, are localized at the periphery of the postsynaptic junctional membrane of principal neurons in the hippocampus and the cerebellum [19, 20]. Our time-lapse recording of TLS-GFP revealed that treatment with DHPG, a selective group 1 mGluR agonist, increased the amount of TLS-GFP clusters in the spines of mature dendrites within 30 min of stimulation (Figure 3). By using hippocampal neurons from mGluR5 knockout mice, we showed that postsynaptic mGluR5-mediated signaling system was responsible for the translocation of TLS. The reversal of TLS translocation after DHPG washout, shown in Figure 3H, clearly indicates that accumulation of TLS in spines was maintained by mGluR activity and not stabilized by other molecular interactions. Activated postsynaptic mGluR5 can induce increases in both intracellular calcium concentration $[Ca^{2+}]i$ and PKC activation through the G protein-linked inositol phospholipids pathway [21]. On the other hand, PKC activation has been shown to control the redistribution of a wide variety of proteins localized in the postsynaptic density (PSD) [22, 23]. Because PKC is responsible for the reorganization of the actin cytoskeleton in a variety of cell types [24], activation of PKC by mGluR5 may subsequently release TLS-containing RNA granules from their actin bound state and initiate their translocation into spines. This hypothesis can be tested by experiments with multiple fluorescent reporters to simultaneously monitor translocation of TLS and reorganization of the actin cytoskeleton.

Although DHPG treatment induces accumulation of TLS, signaling via mGluR5 cannot be the sole mechanism of TLS accumulation in spines. The presence of

another signaling system is evident from phenotypic examination of cultured neurons from mGluR5 null mice, where transition of TLS from dendritic shafts to spines took place with a time course similar to that for wild-type mice (unpublished data). On the other hand, absence of TLS in hippocampal neurons affected the morphology of the dendrites and reduced the number of the spines (Figure 4). It is likely that accumulation of TLS into spines is essential for their structural maturation but is dependent on multiple signaling systems including mGluR5 activation. Abnormal spine morphology has also been reported in FMRP null mice [25, 26]. In the FMRP knockout mice, neuronal dendrites exhibited long and thin dendritic spines with increased density. This increased spine density may be attributed to the absence of an activity-dependent translational suppression by FMRP [27]. The contrasting phenotypes of these null mutants illustrate the functional diversity of RNA binding proteins in dendrites.

Considering the dual functions of TLS as the RNA-splicing factor and an RNA transporter, we may speculate that TLS may coordinately regulate the rate of RNA splicing in the nucleus and the amount of mRNA transported to local translational machinery in spines in response to synaptic activation. Understanding how postsynaptic metabotropic signals regulate TLS dynamics will be essential in order to decipher the complex cellular system that integrates synaptic activity, RNA splicing and transport, and local dendritic translation. Our present and future findings on the neuronal functions of TLS do and will provide important keys for further understanding the molecular basis of synaptic plasticity and a general insight into local translation in polarized cells.

Supplemental Data

Supplemental Data include four figures, two movies, and Supplemental Experimental Procedures and are available with this article online at http://www.current-biology.com/cgi/content/full/15/6/587/DC1/.

Acknowledgments

We thank M. Kuno, T. Manabe, and H. Sabe for their helpful discussions. We greatly thank D. Ron and E. Schuman for the human TLS and the rat Staufen cDNA clones, respectively. We appreciate T. Ebihara and K. Sobue for kindly providing us CortBP antibody and J. Roder for the generous contribution of mGluR5-null mice. Finally, we thank Y. Sakakida and Y. Watanabe for mouse maintenance as well as K. Hamajima, I. Kawabata, and N. Takashima for their help with preparing the primary cultures of neurons. This work was supported in part by grants from the Ministry of Education, Culture, Sports, Science and Technology, Mitsubishi Pharma Research Foundation, Senri Life Science Foundation, and Sony Corporation. G.G.H. was supported by grants from the National Cancer Institute of Canada.

Received: September 1, 2004
Revised: January 5, 2005
Accepted: January 5, 2005
Published: March 29, 2005

References

1. Hering, H., and Sheng, M. (2001). Dendritic spines: structure, dynamics and regulation. Nat. Rev. Neurosci. *2*, 880–888.
2. Kiebler, M.A., and DesGroseillers, L. (2000). Molecular insights into mRNA transport and local translation in the mammalian nervous system. Neuron *25*, 19–28.
3. Job, C., and Eberwine, J. (2001). Localization and translation of mRNA in dendrites and axons. Nat. Rev. Neurosci. *2*, 889–898.
4. Steward, O., and Schuman, E.M. (2001). Protein synthesis at synaptic sites on dendrites. Annu. Rev. Neurosci. *24*, 299–325.
5. Steward, O., and Schuman, E.M. (2003). Compartmentalized synthesis and degradation of proteins in neurons. Neuron *40*, 347–359.
6. Crozat, A., Aman, P., Mandahl, N., and Ron, D. (1993). Fusion of CHOP to a novel RNA-binding protein in human myxoid liposarcoma. Nature *363*, 640–644.
7. Iko, Y., Kodama, T.S., Kasai, N., Oyama, T., Morita, E.H., Muto, T., Okumura, M., Fujii, R., Takumi, T., Tate, S., et al. (2004). Domain architectures and characterization of an RNA-binding protein, TLS. J. Biol. Chem. *279*, 44834–44840.
8. Zinszner, H., Sok, J., Immanuel, D., Yin, Y., and Ron, D. (1997). TLS (FUS) binds RNA in vivo and engages in nucleo-cytoplasmic shuttling. J. Cell Sci. *110*, 1741–1750.
9. de Hoog, C.L., Foster, L.J., and Mann, M. (2004). RNA and RNA binding proteins participate in early stages of cell spreading through spreading initiation centers. Cell *117*, 649–662.
10. Husi, H., Ward, M.A., Choudhary, J.S., Blackstock, W.P., and Grant, S.G. (2000). Proteomic analysis of NMDA receptor-adhesion protein signaling complexes. Nat. Neurosci. *3*, 661–669.
11. Kanai, Y., Dohmae, N., and Hirokawa, N. (2004). Kinesin transports RNA; isolation and characterization of an RNA-transporting granule. Neuron *43*, 513–525.
12. Kohrmann, M., Luo, M., Kaether, C., DesGroseillers, L., Dotti, C.G., and Kiebler, M.A. (1999). Microtubule-dependent recruitment of Staufen-green fluorescent protein into large RNA-containing granules and subsequent dendritic transport in living hippocampal neurons. Mol. Biol. Cell *10*, 2945–2953.
13. Tang, S.J., Meulemans, D., Vazquez, L., Colaco, N., and Schuman, E. (2001). A role for a rat homolog of staufen in the transport of RNA to neuronal dendrites. Neuron *32*, 463–475.
14. Kang, H., and Schuman, E.M. (1996). A requirement for local protein synthesis in neurotrophin-induced hippocampal synaptic plasticity. Science *273*, 1402–1406.
15. Schratt, G.M., Nigh, E.A., Chen, W.G., Hu, L., and Greenberg, M.E. (2004). BDNF regulates the translation of a select group of mRNAs by a mammalian target of rapamycin-phosphatidylinositol 3-kinase-dependent pathway during neuronal development. J. Neurosci. *24*, 7366–7377.
16. Lu, Y.M., Jia, Z., Janus, C., Henderson, J.T., Gerlai, R., Wojtowicz, J.M., and Roder, J.C. (1997). Mice lacking metabotropic glutamate receptor 5 show impaired learning and reduced CA1 long-term potentiation (LTP) but normal CA3 LTP. J. Neurosci. *17*, 5196–5205.
17. Hicks, G.G., Singh, N., Nashabi, A., Mai, S., Bozek, G., Klewes, L., Arapovic, D., White, E.K., Koury, M.J., Oltz, E.M., et al. (2000). Fus deficiency in mice results in defective B-lymphocyte development and activation, high levels of chromosomal instability and perinatal death. Nat. Genet. *24*, 175–179.
18. Sholl, D.A. (1953). Dendritic organization in the neurons of the visual and motor cortices of the cat. J. Anat. *87*, 387–406.
19. Baude, A., Nusser, Z., Roberts, J.D., Mulvihill, E., McIlhinney, R.A., and Somogyi, P. (1993). The metabotropic glutamate receptor (mGluR1 alpha) is concentrated at perisynaptic membrane of neuronal subpopulations as detected by immunogold reaction. Neuron *11*, 771–787.
20. Shigemoto, R., Nomura, S., Ohishi, H., Sugihara, H., Nakanishi, S., and Mizuno, N. (1993). Immunohistochemical localization of a metabotropic glutamate receptor, mGluR5, in the rat brain. Neurosci. Lett. *163*, 53–57.
21. Nakanishi, S. (1994). Metabotropic glutamate receptors: synaptic transmission, modulation, and plasticity. Neuron *13*, 1031–1037.
22. Fong, D.K., Rao, A., Crump, F.T., and Craig, A.M. (2002). Rapid synaptic remodeling by protein kinase C: reciprocal translocation of NMDA receptors and calcium/calmodulin-dependent kinase II. J. Neurosci. *22*, 2153–2164.
23. Lan, J.Y., Skeberdis, V.A., Jover, T., Grooms, S.Y., Lin, Y., Ar-

aneda, R.C., Zheng, X., Bennett, M.V., and Zukin, R.S. (2001). Protein kinase C modulates NMDA receptor trafficking and gating. Nat. Neurosci. *4*, 382–390.

24. Keenan, C., and Kelleher, D. (1998). Protein kinase C and the cytoskeleton. Cell. Signal. *10*, 225–232.
25. Comery, T.A., Harris, J.B., Willems, P.J., Oostra, B.A., Irwin, S.A., Weiler, I.J., and Greenough, W.T. (1997). Abnormal dendritic spines in fragile X knockout mice: maturation and pruning deficits. Proc. Natl. Acad. Sci. USA *94*, 5401–5404.
26. Nimchinsky, E.A., Oberlander, A.M., and Svoboda, K. (2001). Abnormal development of dendritic spines in FMR1 knock-out mice. J. Neurosci. *21*, 5139–5146.
27. Antar, L.N., and Bassell, G.J. (2003). Sunrise at the synapse: the FMRP mRNP shaping the synaptic interface. Neuron *37*, 555–558.